Title

Imaging Sleep-Wake Activity in Identified Pontine Cell Populations

Author

Cox, Julia Mary

Publication Date

2014

Peer reviewed|Thesis/dissertation

Imaging Sleep-Wake Activity in Identified Pontine Cell Populations

By

Julia Mary Cox

A dissertation submitted in partial satisfaction of the

requirements for the degree of

Doctor of Philosophy

in

Vision Science

in the

Graduate Division

of the

University of California, Berkeley

Committee in charge:

Professor Yang Dan, Chair
Professor Hillel Adesnik
Professor Michael Silver

Fall 2014

Abstract

Imaging Sleep-Wake Activity in Identified Pontine Cell Populations

by

Julia Mary Cox

Doctor of Philosophy in Vision Science

University of California, Berkeley

Professor Yang Dan, Chair

An animal's level of arousal transitions rapidly and repeatedly over the course of a day, corresponding with changes in global patterns of neural activity. Decades of research have identified distinct brain regions responsible for the induction and maintenance of sleep and wake states but it has been difficult to determine the precise role of specific neuronal subtypes within these regions. The laterodorsal tegmental nucleus (LDT) in the brainstem is one of the structures important for the induction and maintenance of both rapid eye movement (REM) sleep and wakefulness, and is comprised of multiple, intermingled cell types. In order to characterize the brain state-specific activity of identified neurons in this region, we transfected GABAergic or glutamatergic neurons with the calcium indicator GCaMP6s. We then imaged their activity using a microendoscope and head mountable fluorescence microscope in the feely moving mouse as it transitioned naturally through the sleep wake cycle. This technique allowed us to monitor the activity of multiple cells simultaneously and define their state specific-activity patterns. The populations of both GABAergic and glutamatergic neurons had heterogeneous response properties, but were primarily active during periods of REM, wakefulness or both. Furthermore, changes in the activity of these neurons anticipate transitions in global brain state and the pattern of activation varies depending on the cell's position within the LDT. These results indicate that different cell types within the LDT are modulated by the sleep-wake cycle and may have distinct roles in the regulation of brain state.

Table of Contents

Acknowledgements

I would like to thank my advisor, Yang Dan, for her scientific guidance and for providing me with countless opportunities to explore and learn over the years. I would also like to thank my thesis committee, Michael Silver and Hillel Adesnik, for their valuable insight as I prepared this dissertation.

I would like to thank the members of the Dan lab for teaching me the skills I needed for this research and for many useful discussions. I'd especially like to acknowledge Shinjae Chung and Franz Weber for always answering my questions and Lucas Pinto for much help with data analysis. I would also like to thank Shannon Leslie and Corrina Elder for their technical assistance.

It has been inspiring to be part of the Vision Science Graduate Program, and I would like to thank this immensely supportive and passionate group of students and faculty.

I would like to thank my parents for being the first to show me that science is fun and believing I was good at it, and for their continual encouragement and support. Finally, thanks to Lucas not only for all his scientific help but his tireless encouragement as well.

Chapter 1. Introduction: Brainstem mechanisms of sleep and wakefulness

1.1 The sleep-wake cycle

An animal's behavioral state transitions rapidly and repeatedly over the course of a day in response to changing external and internal stimuli. For instance, behavioral states can reflect engagement in a cognitive task or a general level of arousal, and this global brain state can in turn effect cognitive performance and the processing of sensory stimuli (Gervasoni 2004; Gilbert & Sigman 2007; Hurley et al. 2004; Lee & Dan 2012; Pinto et al. 2013; Poulet & Petersen 2008).

Although not all animals fulfill all the criteria of the mammalian sleep-wake cycle, fluctuations in brain state have been found throughout the animal kingdom. No species has been identified that definitively lacks sleep, defined as a period of easily reversible behavioral quiescence accompanied by decreased responsiveness to sensory stimuli (Cirelli & Tononi 2008). Another important feature of sleep that is shared across most species is that it is homeostatically regulated. When sleep is prevented, sleep pressure increases and ultimately sleep rebound occurs. This is a period of increased sleep time, elevated arousal thresholds, and enhanced amounts of slow wave EEG activity (Borbély & Neuhaus 1979; Huber et al. 2000; Huber et al. 2004; Siegel 2005; Vyazovskiy et al. 2011). Despite its ubiquity, however, the underlying mechanisms of brain state regulation remain incompletely understood.

Distinct behavioral states are associated with different patterns of global neural activity that are reflected in the cortical electroencephalogram (EEG), and can be broadly divided into three stages: wake, non-rapid eye movement (NREM) sleep and rapid eye movement (REM) sleep. Wake is associated with high frequency, low-voltage oscillations in the EEG and is accompanied by elevated muscle tone, measured with electromyography (EMG). The onset of NREM sleep, in contrast, brings slower, higher amplitude EEG oscillations and decreased muscle tone. A distinct state of sleep is REM sleep, which is characterized by high frequency, low amplitude, wake-like EEG activity, but unlike wakefulness is accompanied by a near absence of muscle tone (Figure 1.1) (Gervasoni 2004; Timo-Iaria et al. 1970; Van Twyver 1969).

Identifying the structures necessary for the generation of these brain states began in the early 20th century with a neurologist named Constantin von Economo who treated a group of patients suffering from what came to be known as *encephalitis lethargica*. This encephalitis specifically damaged regions of the brain involved in the regulation of sleep and arousal, resulting either in pronounced insomnia or somnolence. The group of patients who slept excessively had lesions at the junction of the brainstem and posterior hypothalamus, leading von Economo to propose that the brainstem contains an

ascending arousal system that activates the forebrain. The other group of patients had difficulty falling asleep and could only stay asleep for short periods of time. These patients had lesions in the basal ganglia and anterior hypothalamus, suggesting that these regions were important for the onset and maintenance of sleep (Triarhou 2006; von Economo 1930). Subsequently, a distributed network of nuclei within the brainstem, hypothalamus and basal forebrain has been confirmed as vital to the regulation of the sleep-wake cycle.

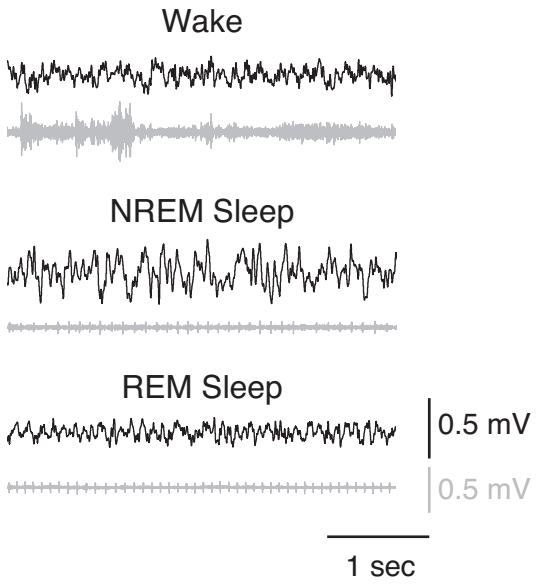

Figure 1.1: Example EEG and EMG from a period of wake, NREM sleep and REM sleep

1.2 Brainstem mechanisms of arousal

In mammals, there are multiple, overlapping neural systems that promote arousal, and activation of these various elements contributes to specific features of the complex state of wakefulness. The brainstem maintains wakefulness via two separate pathways: an ascending projection to the basal forebrain, hypothalamus, thalamus and cortex perpetuates cortical activation, while a descending pathway to the spinal cord maintains muscle tone (Holstege & Kuypers 1987; Jones 2008; Jones & Yang 1985). Consistent with the lesion locations of von Economo's somnolent patients, Moruzzi and Magoun found that electrical stimulation of the midbrain reticular formation resulted in persistent desynchronization (the decrease of high amplitude, low frequency activity and increase in low amplitude, high frequency EEG activity typical of wakefulness) of the cortical EEG (Moruzzi & Magoun 1949), supporting the idea that sustained input from the brainstem to the forebrain is important for arousal. Stimulation of

this structure remains one of the most reliable ways to induce signs of cortical arousal, and many neurons within this structure are most active during periods of cortical desynchronization (wake and REM) (Steriade et al. 1982).

The ascending reticular activating system is comprised of multiple nuclei broadly located within the midbrain and pons. These structures project along two major pathways: a dorsal pathway to the thalamocortical projection system and a ventral pathway to the lateral hypothalamus and basal forebrain, from which other neurons project to cortex, promoting desynchronization of cortical EEG and arousal (Jones & Yang 1985). The wake promoting structures of the brainstem include glutamatergic neurons of the pons and midbrain, cholinergic neurons from the pedunculopontine and laterodorsal tegmental nuclei (PPT, LDT), noradrenergic locus coeruleus (LC) neurons, and serotonergic dorsal (DR) and median raphe (MR) neurons (Figure 1.2) (Brown et al. 2012; Cornwall & Phillipson 1988; Hallanger et al. 1987; Steriade et al 1982; Steriade et al. 1988; Jones & Yang 1985; Loughlin et al. 1986).

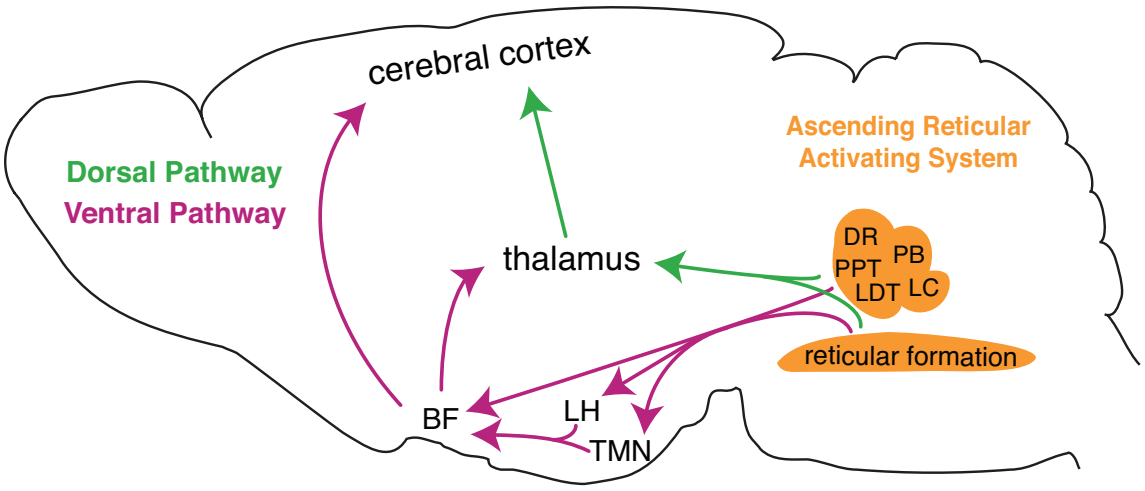

Figure 1.2: Schematic of the Ascending Reticular Activating System. The DR serotonergic neurons, PPT/LDT cholinergic neurons, noradrenergic LC neurons, glutamatergic PB neurons and the reticular formation comprise the major structures of the ascending reticular activating system. These neurons project along a dorsal and ventral pathway to promote wakefulness in the forebrain. The dorsal pathway perpetuates cortical arousal through direct projections to the thalamus, while the ventral pathway projects to the hypothalamus and basal forebrain (BF), which projects to cortex. BF: basal forebrain; DR: dorsal raphe; LC: locus coeruleus; LDT: laterodorsal tegmental nucleus; LH: lateral hypothalamus; PB: parabrachial nucleus; PPT: pedunculopontine tegmental nucleus; TMN: tuberomamillary nucleus

One population of glutamatergic neurons important for the maintenance of arousal is found in the parabrachial nucleus (PB) and nearby precoeruleus region (Kaur et al. 2013). Cell body-specific lesions to the sub-nuclei of the PB increase sleep time while a lesion of the entire area induces a comatose state (Fuller et al.

2011). Furthermore, a group of neurons positioned more rostrally are known to be important for the regulation of forebrain arousal and the initiation of movement. Optogenetic stimulation of these glutamatergic neurons results in the rapid induction of locomotion and a concomitant increase in low amplitude, high frequency local field potential (LFP), typical of active wakefulness. Furthermore, stimulation at a level not sufficient to induce movement similarly affects the LFP, suggesting that these neurons are directly involved in the modulation of both cortical state and the generation of movement (Lee et al. 2014).

Noradrenergic LC neurons send diffuse projections throughout the brain, including to cortex, the hippocampus, amygdala, thalamus, hypothalamus and basal forebrain (Berridge 2008; Dahlström & Fuxe 1964; Foote et al. 1983; Sara 2009). Single unit recordings from the LC reveal them to be maximally active during wake, less active during NREM sleep and practically silent during REM sleep (Aston-Jones & Bloom 1981; Takahashi et al. 2010). Furthermore, optogenetic stimulation of noradrenergic LC neurons causes a rapid transition into wake, while sustained optogenetic inhibition of these neurons increases sleep time (Carter et al. 2010). LC neurons are also thought to be important for the maintenance of muscle tone during wakefulness. In addition to their diverse forebrain projections, noradrenergic LC neurons project to the spinal cord (Reddy et al. 1989), and stop firing completely with the loss of muscle tone that happens during cataplexy (Burgess & Peever 2013; Wu et al. 1999). This supports the hypothesis that the cessation of LC activity is necessary for the induction of muscle atonia and REM sleep. Another major monoaminergic population thought to be important for the maintenance of arousal is the serotonergic DR. These neurons also project widely and are maximally active during wake, progressively decreasing their firing rate through NREM sleep until they are nearly silent during REM (McGinty & Harper 1976; Monti 2011).

The brainstem cholinergic neurons important for brain state regulation are clustered in the LDT and PPT (Armstrong et al. 1983). Anterograde and retrograde tracing studies combined with choline acetyltransferase (ChAT) immunohistochemistry have revealed extensive cholinergic projections to nearly every thalamic nucleus, the hypothalamus and basal forebrain. These neurons do not project directly to cortex, instead mediating cortical desynchronization via input to thalamocortical projection neurons and the basal forebrain (Hallanger et al. 1987; Paré et al. 1988; Semba et al. 1990; Steriade 2004). Single-unit electrophysiology experiments reveal that cholinergic brainstem neurons increase their activity not only during wake, but during REM sleep as well, suggesting that their activity is important for cortical desynchronization regardless of arousal level (Boucetta et al. 2014; Datta & Siwek 2002; Sakai 2012).

1.3 Brainstem mechanisms of REM sleep

As suggested by the sleep-wake activity profile of cholinergic neurons, the brainstem has been implicated in the generation of REM sleep as well as

arousal. Aserinsky and Kleitman first described REM sleep in 1953 when they quantitatively monitored eye movements with electrooculograms in combination with EEG recordings in sleeping subjects. They described a stage of sleep characterized by rapid, binocularly symmetrical eye movements, which were accompanied by a reduction of the low frequency, high voltage EEG typical of other stages of sleep, in favor of low amplitude, high frequency EEG. This pattern of EEG activity is very similar to that seen during wake, which led some to call this stage of sleep paradoxical sleep. They further discovered that most subjects described detailed dreams involving visual imagery after being awakened during this stage of sleep (Aserinsky & Kleitman 1953). Another cardinal feature of REM sleep is a dramatic suppression of muscle tone (Siegel 2013), and hippocampal theta (7-12 Hz) activity is prominent, especially in rodents (Robinson et al. 1977). In addition to these tonic features of REM sleep, electrical potentials known as ponto-geniculo-occipital waves (PGO waves) also appear during REM. PGO waves originate in the pons and are then propagated to the lateral geniculate nucleus and on to occipital cortex. They occur as isolated, spiky, high-amplitude potentials and are usually associated with rapid eye movements (Malcolm et al. 1970; Shouse & Siegel 1992).

Identification of REM-promoting structures: Some of the earliest clues to the location of REM-generating brain regions came from transection studies in the cat. When the forebrain is severed at the rostral border of the superior colliculus, tonic muscle rigidity emerges as soon as the animal is removed from anesthesia. Periodically, however, this contraction relaxes in a manner consistent in rhythmicity and duration with the muscle atonia of REM sleep. Jouvet and colleagues combined these transections with EMG, EEG and eye movement recordings and evaluated any persisting sleep-wake activity in the isolated brain regions. After separation from the brainstem, they found that the forebrain no longer showed any signs of REM sleep, displaying persistently high voltage EEG activity and no PGO-waves in the cortex or thalamus. Behind the transection, in the midbrain and brainstem, however, signs of REM sleep persisted; muscle atonia was accompanied by PGO spikes recorded in the pons with similar periodicity and duration to that seen in the intact animal (Jouvet 1967).

If the transection instead severs the connection between the brainstem and spinal cord, all features of REM sleep, except for muscle atonia, are present (Adey et al. 2008; Siegel 2013). The REM sleep generator was further localized by separating the caudal pons from the medulla. In this case no muscle atonia is evident, although electrical stimulation of the medulla is still sufficient to suppress muscle tone in decerebrate cats. This experiment suggests that the medulla is required for the expression of muscle atonia, but is dependent on activation from some more rostral region (Lai & Siegel 1988). The regions anterior to the transection still showed signs of REM sleep, namely PGO waves measurable in both the pons and the forebrain, comparable to those seen in the intact animal (Jouvet 1967; Siegel et al. 1984; Siegel et al. 1986). Furthermore, if the pons and

caudal midbrain are separated from the forebrain as well as the medulla and spinal cord, features of REM are still evident in the isolated pons, but no signs of REM sleep are found in either the rostral or caudal regions (Matsuzaki 1969).

These studies suggest that although some of the features of REM sleep are realized by circuitry within the forebrain or caudal brainstem and spinal cord, the pons is the only region that is sufficient to generate signs of REM sleep in isolation. More localized lesions in the pons and caudal midbrain identified several regions within the pontine reticular formation (PRF) important for the generation of REM sleep and its various features. Large lesions in this area resulted in decreased REM sleep**,** whereas smaller lesions effected individual REM features, such as muscle atonia (Vertes 1984).

One of the primary regions implicated in pontine REM-sleep control has been variously named. In the cat it is called the subcoeruleus (subC), which is located immediately ventral to the noradrenergic core of the LC. A smaller region within the subC, called the peri-LCα, contains neurons involved in muscle atonia. In the rodent, the structure that is considered functionally equivalent to the subC is the sublaterodorsal nucleus (SLD) which is positioned slightly more rostral and ventral than the SubC (Brown et al. 2012; Krenzer et al. 2011; Lu et al. 2006; Luppi et al. 2006;). Complementing the results of the lesion studies, a large number of neurons were recorded in this region that were tonically and specifically active during REM sleep (Clément et al. 2011; Hobson et al. 1975; Shiromani et al. 1992; Verret et al. 2005; Yamamoto et al. 1990).

Pontine mechanisms of REM sleep generation: Theories regarding the circuitry underlying the induction and maintenance of REM sleep within the pons generally posit the existence of two reciprocally connected populations of neurons: REM-on neurons and REM-off neurons. The identity and precise location of these different populations of neurons is still under investigation, however.

The earliest theories proposed that transitions in and out of REM are mediated by the reciprocal interaction of the cholinergic and monoaminergic systems in the pons (Hobson et al. 1975). The cholinergic cells were hypothesized to be REM promoting while the monoaminergic cells were REM inhibiting. Supporting the REM-inhibiting role of monoaminergic systems, serotonergic and noradrenergic brainstem neurons have been shown to be most active during wake and essentially inactive during REM sleep (Aston-Jones & Bloom 1981; McGinty & Harper 1976; Takahashi et al. 2010). Furthermore, *in vitro* experiments have shown that norepinephrine hyperpolarizes brainstem cholinergic neurons via α2-adrenoreceptors, suggesting they may inhibit the REM-promoting cholinergic neurons (Williams & Reiner 1993).

The involvement of the cholinergic system in REM sleep generation was demonstrated by the injection of carbachol, a cholinergic agonist, into specific regions of the pons. Depending on the precise location of the injection, carbachol infusions were sufficient to induce REM sleep or isolated REM features

(Baghdoyan, Monaco, et al. 1984a; Baghdoyan, Rodrigo-Angulo, et al. 1984b; George et al. 1964; Gnadt & Pegram 1986; Siegel 2013; Yamamoto et al. 1990). In addition, neurotoxic destruction of cholinergic neurons in the pons led to a decrease in REM sleep (Webster & Jones 1988) and microdialysis studies revealed increased release of acetylcholine in the cortex, hippocampus, pons and medulla during REM sleep compared to NREM sleep (Kodama et al. 1990; Kodama et al. 1998; Marrosu et al. 1995). In light of these experimental findings suggesting the importance of acetylcholine in the generation of REM sleep, it was hypothesized that the cholinergic neurons in the brainstem were the REM-on neurons posited to mediate REM-NREM transitions. When the activity of individual cholinergic neurons was monitored electrophysiologically, however, these neurons were found to be active during both REM and wake, not specifically during REM (Boucetta et al. 2014; Kayama et al. 1992; Sakai 2012; Datta & Siwek 2002). Ultimately, in rats it was shown that the REM-on neurons in the SLD were not cholinergic (Lu et al. 2006). Thus, although there is a great deal of evidence supporting the involvement of the cholinergic system in the onset and maintenance of REM, it seems likely that other neurotransmitter systems are involved as well.

For instance, in the region of the subC optimal for carbachol-induced REM, only 50% of the REM-on neurons are sensitive to the cholinergic agonist (Yamamoto et al. 1990), suggesting the existence of additional excitatory input to the subC. In fact, there is evidence that glutamatergic innervation of the subC/SLD region is also important for REM sleep. Infusion of non-NMDA glutamate receptor agonists into the carbachol-sensitive pontine region of cats leads to muscle atonia (Lai et al. 1993), and injection of a glutamate agonist in the SLD induces REM sleep in rats (Boissard et al. 2002). Moreover, after a period of enhanced REM following REM sleep deprivation, many of the LDT and SLD neurons labeled with *Fos* are glutamatergic (Clément et al. 2011), further suggesting a population of REM-on glutamatergic neurons in the pons.

REM-on GABAergic neurons are also likely to play a role in the generation of REM sleep via the inhibition of REM-off populations. For instance, microdialysis studies show an increase in GABA levels in the REM-off LC during REM sleep compared to wake (Nitz & Siegel 1997). The LC receives strong input from GABAergic neurons in the paragigantocellular nucleus in the medulla (Cedarbaum & Aghajanian 1978; Luppi et al. 1995; Sapin et al. 2009), where single unit recordings and *Fos* staining have revealed populations of REM-on neurons (Goutagny et al. 2008; Sapin et al. 2009), which could potentially inhibit LC activity during sleep.

There is also evidence that in addition to the monoaminergic neurons, GABAergic mechanisms are also involved in the antagonism of REM sleep. Injection of $GABA_A$ receptor antagonists into the SLD causes an increase in the amount of REM sleep, suggesting that the REM-on neurons of the SLD may be

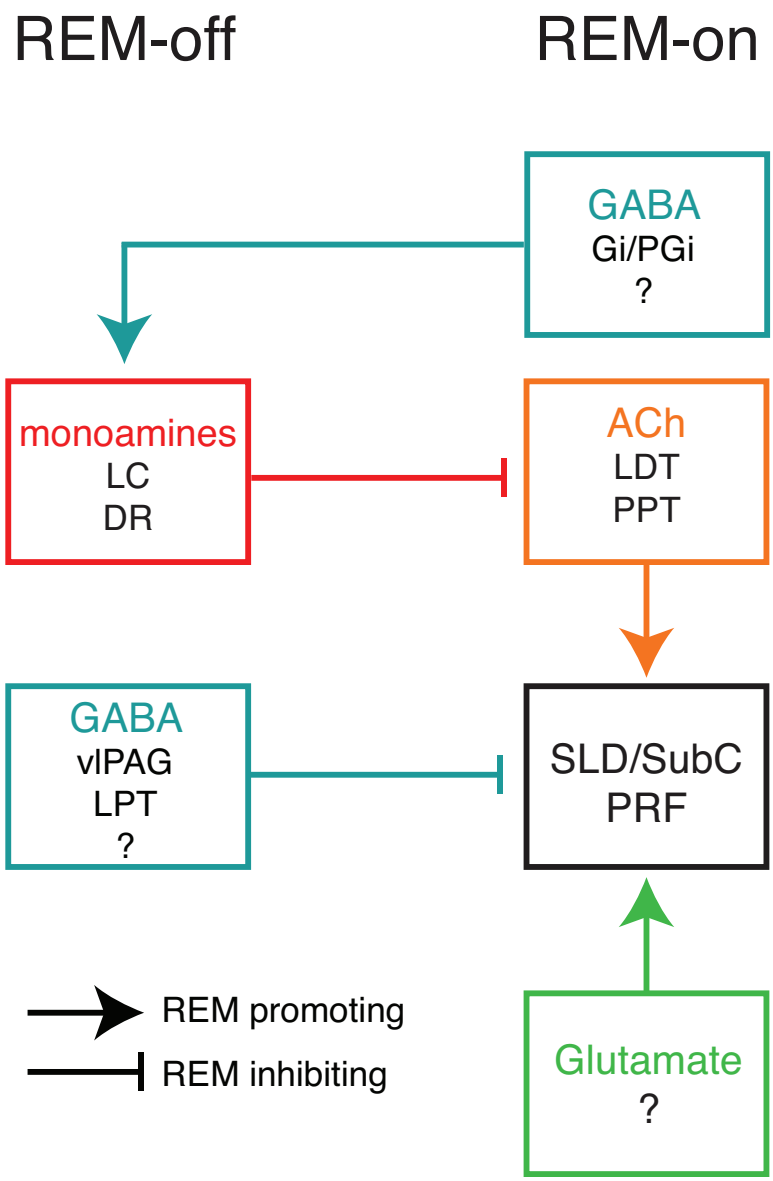

Figure 1.3: The relationship between different neurotransmitter systems in the generation of REM sleep. Based on pharmacology, *Fos* staining, electrophysiology and lesion studies, the REM promoting and REM inhibiting actions of various neurotransmitter systems on the REM-producing SLD/SubC and pontine reticular formation (PRF) is schematized. The source of relevant glutamatergic and GABAergic input is not yet entirely known, but identified sources are labeled. ACh: acetylcholine; DR: dorsal raphe; Gi: gigantocellular reticular nucleus; LC: locus coeruleus; LDT: laterodorsal tegmental nucleus; LPT: lateral pontine tegmentum; PGi: paragigantocellular nucleus; PPT: pedunculopontine tegmental nucleus; PRF: pontine reticular formation SLD: sublaterodorsal tegmental nucleus; SubC: subcoeruleus; vlPAG: ventrolateral periaqueductal gray

tonically inhibited during wake and slow wave sleep (Boissard et al. 2002; Pollock & Mistlberger 2003; Luppi et al. 2006; Sanford et al. 2003). Supporting this idea, microdialysis experiments revealed that levels of GABA in this region are greater during wakefulness than during REM (Vanini et al. 2011). Furthermore, injection of GABA or $GABA_A$ receptor agonists into the cholinoceptive region of the pons increases wakefulness, and blocks carbachol induced REM (Xi et al. 1999; Xi et al. 2004). It has been further posited based on *Fos* studies combined with immunohistochemistry and anatomical tracing, that the REM-inhibiting GABAergic input to the SLD comes from the more anterior ventrolateral periaqueductal gray (vlPAG) and lateral pontine tegmentum (Lu et al. 2006; Sapin et al. 2009). Accordingly, pharmacological inhibition (Sapin et al. 2009) or cell body specific lesions of these areas cause an increase in REM sleep (Lu et al. 2006).

Although there is clear evidence for the involvement of cholinergic, monoaminergic, glutamatergic and GABAergic mechanisms in the generation and maintenance of REM sleep, the precise locations and connectivity of these neuronal populations is still to be ascertained. Figure 1.3 shows a hypothetical schematic of the interactions between these different populations based on the experimental data presented above.

1.4 The laterodorsal tegmental nucleus

As described above, the cholinergic system is known to be critically involved in multiple elements of the sleep-wake cycle. Cholinergic neurons are active during both REM and wake and are involved in the desynchronization of cortical activity, a feature common to these two brain states. Based on pharmacology and lesion studies, however, there is evidence that the cholinergic system is involved in REM-specific features as well, such as the production of muscle atonia and PGO-wave generation (Baghdoyan, Rodrigo-Angulo, et al. 1984b; Brown et al. 2012; George et al. 1964; Gnadt & Pegram 1986; Shouse & Siegel 1992). Cholinergic brainstem neurons send descending projections to various regions of the brainstem implicated in REM sleep such as the SLD and medulla (Woolf & Butcher 1989; Lai et al. 1993). Interestingly, a subset of these cholinergic neurons project to both the thalamus and the cholinoceptive pontine regions (Semba et al. 1990), suggesting that the same cholinergic neuron may be involved in cortical desynchronization and other REM-specific features. How exactly the REM-specific actions of these neurons are suppressed during wake is not clear, but may involve GABAergic or monoaminergic inhibition of REM-promoting targets of the LDT and PPT cholinergic neurons. In fact, systemic administration of an anti-acetylcholinesterase induces REM sleep only when accompanied by the depletion of monoamines, suggesting the removal of monoaminergic inhibition is necessary for the cholinergic expression of REM sleep (Karczmar et al. 1970).

The LDT and PPT are not homogenously cholinergic, however, but are

instead comprised of intermingled GABAergic, glutamatergic and cholinergic neurons (Clements & Grant 1990; Ford et al. 1995; Wang & Morales 2009). Although they have not been studied as extensively as the cholinergic neurons, there is evidence that non-cholinergic cells from the PPT/LDT also project to the thalamus and basal forebrain (Hallanger et al. 1987; Paré et al. 1988; Steriade et al. 1988) and send descending projections along with the cholinergic neurons (Semba et al. 1990). Furthermore, identified GABAergic LDT neurons project to the lateral hypothalamus (Ford et al. 1995) and identified glutamatergic LDT neurons were found to project to the subC in cats (Lai et al. 1993), suggesting they may also be involved in the regulation of the sleep-wake cycle. When examined for the presence of *Fos* after a period of enhanced REM sleep, a greater number of non-cholinergic neurons were labeled in the LDT than cholinergic neurons (Verret et al. 2005). Both cholinergic and non-cholinergic neurons have been identified in head restrained mice that are active during REM and wake as well as non-cholinergic neurons that are purely wake active (Sakai 2012). Immunohistochemically defined GABAergic and glutamatergic neurons have also been recorded in the LDT region of head restrained rats that have brain state-modulated activity (Boucetta et al. 2014). These experiments suggest that non-cholinergic neurons of the LDT are involved in the regulation of the sleep-wake cycle.

1.5 Summary and motivation

Previous work has elucidated a role for brainstem GABAergic, glutamatergic, cholinergic and monoaminergic signaling in the regulation of sleep-wake behavior. Although the specific connections between some of these systems have been interrogated, the precise location and connectivity of these neuronal populations, particularly those important for the regulation of REM sleep, have not been fully identified. The LDT is one of the primary sources of brainstem acetylcholine, but this nucleus contains intermingled glutamatergic and GABAergic neurons as well. Primarily due to technical limitations, our understanding of the function of non-cholinergic LDT neurons in brain state regulation is incomplete (but see Boucetta et al. 2014; Sakai 2012; Verret et al. 2005).

In order to assess the sleep-wake activity of LDT neuronal subpopulations, the present work used microendoscope calcium imaging with a genetically encoded calcium indicator to monitor the activity of multiple, identified neurons in the freely moving mouse as it transitioned naturally through the sleep-wake cycle. In addition to clarifying the brain state modulation of non-cholinergic neurons in the LDT region, the present study sought to determine whether these subpopulations could be providing some of the REM-promoting glutamatergic or the REM promoting and/or inhibiting GABAergic drive suggested by previous research. If these neurons can be classified as REM-on or REM-off, it suggests that they may be providing some of the REM-promoting or REM-inhibiting input to

structures outside of the LDT. Another possibility is that the GABAergic neurons are primarily local interneurons responsible for the inhibition of the REM- and wake-active cholinergic neurons in the LDT during NREM sleep. If this were the case, they would be expected to fire maximally during NREM sleep.

In addition to classifying the sleep-wake activity profile of the non-cholinergic neurons, we were interested in determining whether they form homogenous populations. Microendoscope imaging allows us to monitor a larger population of identified neurons simultaneously. Thus, we can determine if the responses fall into the multiple categories of brain state activity suggested by the actions of these neurotransmitters in the sleep-wake cycle. Moreover, if the responses are heterogeneous, microendoscope imaging allows us to establish if there is any spatial organization of the sleep-wake responses, furthering the understanding of the circuitry of the pontine brain state regulatory system.

Chapter 2. Experimental design

2.1 Preface

An enduring question in the study of the pontine regulation of REM sleep and wake is how specific neuronal subtypes are involved in brain state modulation. Cholinergic, monoaminergic, GABAergic and glutamatergic neurons in the pons and midbrain have all been implicated in the sleep-wake cycle (Aston-Jones & Bloom 1981; Boissard et al. 2003; Carter et al. 2010; Clément et al. 2011; Kodama et al. 1990; Lu et al. 2006; Luppi et al. 2006). Thorough investigation of the activity of different types of neurons in this region has been difficult, however, in part because traditional *in vivo* electrophysiology techniques do not permit unambiguous identification of cell type. Although in some regions of the brain different classes of neurons can be putatively distinguished based on spike waveform properties, this characterization is not fully dependable (Cardin 2012).

Efforts to identify the specific activity patterns of different pontine cell types across the sleep-wake cycle have relied primarily on two methods. Juxtacellular recordings from neurons in the brainstem have been combined with single-cell dye filling and immunohistochemistry to identify cell types *post-hoc* (Boucetta et al. 2014; Sakai 2012), but the yield for this technique is low and does not allow for simultaneous monitoring of multiple neurons. The other disadvantage of this technique is that it requires head-fixation of the subject. Although rodents and primates can be trained to sleep under restraint (Boucetta et al. 2014; Issa & Wang 2008; Sakai 2012), it is possible that the animal's restricted ability to move could mask specific neural responses or interfere with the natural sleep architecture.

Another common method used to probe the activity of different cell types across the sleep-wake cycle is to look for the presence of *Fos* in neurons after an animal spends time in a given behavioral state. *Fos* is the protein product of the immediate early gene, *c-fos*, which is expressed when a neuron becomes active. Transcription of *c-fos* typically occurs within minutes of stimulus application, peaks 30-45 minutes later, and the *Fos* protein has a half-life of about 2 hours (Krukoff 1998; Sagar et al. 1988). Because of the fragmented nature of rodent sleep, resulting in rapid and repeated transitions between states (Van Twyver 1969), these experiments often rely on sleep deprivation and recovery sleep or pharmacologically-induced REM sleep (Lu et al. 2006; Shiromani et al. 1992), which may not be entirely consistent with the natural sleep-wake cycle. Furthermore, given the poor temporal resolution of this technique, it is not possible to look at the more precise timing of a neuron's activity; for instance how it changes around the time of a state transition or whether it is phasically or tonically elevated during a given state.

In vivo calcium imaging allows for the monitoring of multiple, identified

neurons in behaving animals. Using a genetically encoded calcium indicator it is possible to target specific populations of neurons for imaging, allowing identification of cell type *in vivo* (Chen et al. 2013). Until recently, *in vivo* application of both one- and two-photon microscopy has been restricted to superficial brain regions due to imaging depth limitations imposed by photon scattering by the brain tissue (Helmchen & Denk 2005). Microendoscope imaging overcomes this limitation by using a gradient refractive index (GRIN) lens implanted into the brain structure of interest. The GRIN lens relays light from the tissue to a focal plane outside of the brain. A miniaturized fluorescence microscope can then be mounted on the head of an adult mouse to allow for imaging of deep brain structures in freely moving and behaving animals (Ghosh et al. 2011; Barretto & Schnitzer 2012). We combined electroencephalography (EEG) and electromyography (EMG) recordings with microendoscope imaging of calcium activity in GABAergic, glutamatergic and cholinergic neurons in the laterodorsal tegmental nucleus (LDT) in freely moving mice to assess the distinct brain state-dependent patterns of activity in these different classes of neurons.

2.2 Animals and surgery

All procedures were approved by the Animal Care and Use Committee at the University of California, Berkeley. Experiments were performed in adult (2-6 months old) GAD2-IRES-cre mice (Jackson Laboratories, Gad2tm2(cre)Zjh/J, stock number 010802), ChAT-IRES-cre mice (Jackson Laboratories, B6;129S6-Chat<tm1(cre)Lowl>/J, stock number 006410) or Vglut2-IRES-cre mice (Jackson Laboratories, Slc17a6tm2(cre)Lowl/J, stock number 016963)**,** (25-40 g, males and females). The animals were housed in a 12/12-hour light/dark cycle with lights on from 7 am to 7 pm with food and water available *ad libitum*.

To image from the brainstem across the sleep-wake cycle, mice were implanted with EEG and EMG electrodes as well as a microendoscope. For the implantation surgery, mice were anesthetized with isofluorane (1.5-2%) and placed in a stereotaxic frame (David Kopf Instruments, Tujunga, CA). The skull was exposed and cleaned of connective tissue. We then stereotaxically injected 250 nL (in Vglut2-IRES-cre or GAD2-IRES-cre mice) or 500 nL (in ChAT-IRES-cre mice) of AAV1-GCaMP6s (AAV1.Syn.GCaMP6s.WPRE.SV40, Penn Vector Core) (Chen et al. 2013) into the laterodorsal tegmental nucleus (LDT; -5.4 AP, .8 ML, 3 and 3.5 DV) using a borosilicate pipette and Nanoject syringe (Drummond Scientific). A stainless steel headplate was then affixed to the skull using dental cement. A stainless steel screw was implanted 1 mm posterior and 1.5 mm lateral to bregma for EEG recording. A second screw was implanted over the contralateral cerebellum as a reference. EMG electrodes (stainless steel wire loops) were implanted in the neck muscles. All wires were attached to a micro-strip connector that was affixed to the skull with dental cement. Finally, at least 45 minutes after the injection, a microendoscope (GRIN lens, Inscopix, 0.5 mm diameter, NA 0.5, pitch 2) was implanted over the injection site (-5.4 AP, 0.8 ML,

3.0 DV). The mice were given two doses of buprenorphine (0.05 mg/kg of body weight, the first before surgery and the second 6-8 hours later) and one dose of meloxicam (5 mg/kg of body weight, before surgery) for pain management.

Two to 4 weeks after the implantation surgery, mice were anesthetized (1.5% isofluorane) and head-fixed. A miniaturized, single-photon, fluorescence microscope (Inscopix) was lowered over the implanted microendoscope until the GCaMP6 fluorescence was visible under illumination with the microscope's LED. The microscope's baseplate was then secured to the skull with dental cement darkened with carbon powder (Sigma, 484164) for subsequent attachment of the microscope to the head (Ghosh et al. 2011).

2.3 Ca^{2+} imaging and brain state recording

All sleep recordings took place during the light cycle in the mouse's home cage, placed within a sound-attenuating chamber with food and water available *ad libitum*. First, mice were briefly anesthetized with isofluorane in order to focus and attach the microscope to the baseplate. EEG and EMG were recorded using a RHA2000-EVAL amplifier board (Intan Technologies), filtered at 1 Hz to 7.5 kHz and digitized at 25 kHz. Recording began at least 30 minutes after recovery from anesthesia. EEG and EMG were recorded continuously. Fluorescence data was acquired for 5 to 15 sessions of 10-30 minutes in length to sample each brain state over several hours. Imaging was not continuous to prevent excessive bleaching of the calcium indicator. Calcium imaging data was acquired using nVista HD software (Inscopix) at 10-15 frames per second.

2.4 Histology

To confirm the imaging location, mice were deeply anesthetized and transcardially perfused with ~15 mL of PBS followed by ~10 mL of 4% paraformaldehyde (PFA). Imaging locations were identified based on the position of lesions caused by the GRIN lens. To help localize the position of the lesions, we performed either tyrosine hydroxylase (TH) or choline acetyltransferase (ChAT) immunohistochemistry. The brain was removed and post-fixed overnight in 4% PFA, and then placed in a 30% sucrose solution for cryoprotection for 24-48 hours. The brainstem was sectioned in 30 µm thick coronal slices with a cryostat (Leica Microsystems). Slices were washed with PBST (0.2% Triton X-100 in Phospate-buffered saline [PBS]) and incubated for 2 hours with blocking buffer (2% normal donkey serum in PBST for ChAT staining or 2% normal goat serum and 50 mg/mL BSA in PBST for TH staining). The buffer was washed out with PBST and the samples were incubated overnight at 4ºC with primary antibody (1:200 dilution in blocking buffer, goat anti-ChAT IgG antibody, catalog no. AB144P, Millipore; or 1:1000 dilution in blocking buffer of polyclonal rabbit anti-TH antibody, Abcam**)**. Samples were then washed with PBST and incubated

for 2 hours at room temperature with the secondary antibody (1:250 dilution of Alexa Fluor 594 Donkey Anti-goat IgG antibody or 1:1000 dilution Alexa Fluor 594 Goat Anti-Rabbit IgG antibody, both from Invitrogen**).** Slides were mounted using Vectashield with DAPI (Vector Labs). Images were acquired with a Hamamatsu NDP slide scanner (Hamamatsu Nanozoomer 2.0HT).

The positions of the lesions were identified using anatomical landmarks as well as the position of the locus coeruleus as marked by TH immunostaining or the LDT/PPT as marked by ChAT immunostaining.

2.5 Data Analysis

State Classification: Processing of EEG and EMG data was performed using MATLAB (R2014a, MathWorks). EEG and EMG signals were digitally filtered (1 to 100 Hz for EEG and 200-1000 Hz for EMG) and spectrally decomposed by fast Fourier transformation using a 1-second sliding window with 0.5-second steps. We then extracted delta (1-5 Hz), theta (7-10 Hz) and combined EMG (300-500 Hz) power. Brain state was assessed in 10-second epochs (extracted power time series were averaged over a 10-second sliding window with 5-second step). Average delta power, EMG power or theta power/delta power ratio across the entire recording period were used as thresholds for state classification. NREM sleep is characterized by increased slow wave activity and low EMG power, so epochs where the delta power was above threshold while EMG and the theta/delta power ratio were below threshold were classified as NREM. REM sleep is identified by a decrease in low frequency power, very low EMG activity and increased theta power. Epochs were classified as REM if theta/delta power was above threshold, delta power was below threshold and EMG power was below threshold. Finally, wake epochs were classified as periods of above threshold EMG power, above threshold theta/delta power and below threshold delta power. Figure 2.1 shows example EEG and EMG data from all three states as well as an example of the state classification procedure and resulting state identification. If a REM period was detected immediately following a wake period (if for instance EMG power had dropped before the increase in delta power that marks the onset of NREM sleep, thus fitting the hallmarks of REM), the epoch was changed to wake, because in natural sleep the wake to REM transition does not occur.

Processing of Ca^{2+} images: Images were converted and spatially downsampled by 4 pixel bins using the Inscopix Image Decompressor and nVista Viewer (Inscopix). Subsequent processing and analysis of imaging data were performed in MATLAB. To correct for lateral motion of the brain relative to the GRIN lens, we calculated the difference between the image stack and the image stack smoothed with a 20-pixel-radius disk filter. We then selected a high contrast subregion from the mean projection of the new image stack to be used as a reference (Ziv et al. 2013). To register each frame to the reference, we

calculated the cross correlation between the reference image and the corresponding subregion of each frame of the filtered image stack and identified the shift with the maximum correlation. This shift was then applied to the entire frame of the original image stack.

Regions of interest (ROIs) were manually selected from the mean projection of the corrected image stack of the first imaging session of the day. ROIs were aligned across sessions using a semi-automated method whereby the ROIs from the first session were shifted in the x and y direction by up to ± 5 pixels, to maximize the fluorescence within the ROIs. Alignment was then manually corrected as necessary.

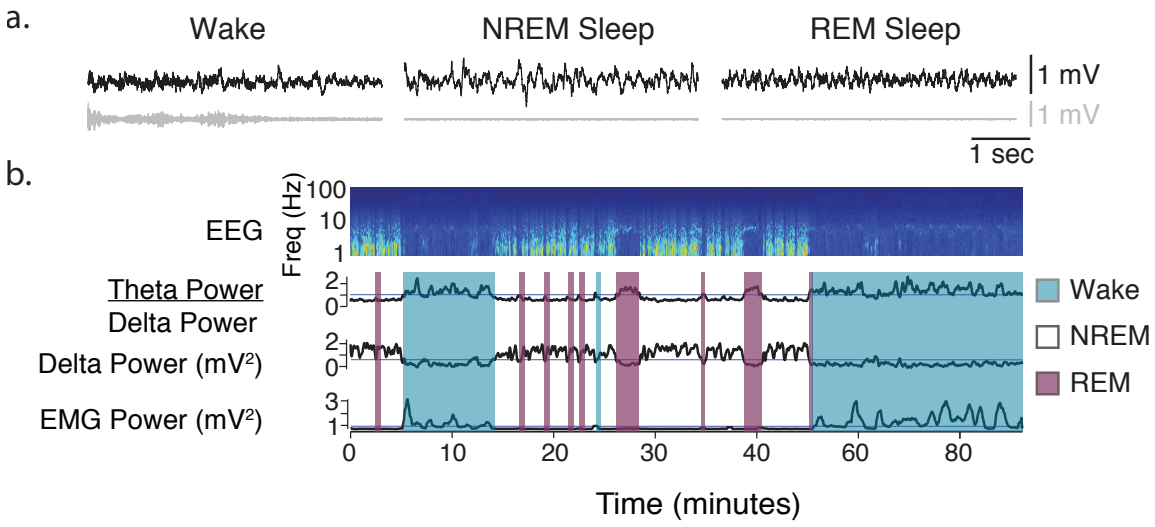

Figure 2.1: State Classification. a) Example EEG and EMG data from all classified brain states. b) An example of state classification based on EEG and EMG recordings. The top panel shows the frequency decomposition of the EEG signal. The delta power and theta power/delta power ratio are extracted from the EEG and used in combination with the EMG power to classify brain state. The results of the brain state classification are overlaid on the EEG and EMG signals.

Fluorescence analysis: The pixels within each ROI were averaged to create a fluorescence time series. To remove contamination from surrounding neuropil, we extracted the fluorescence from a ring-shaped region with a width of 10 µm from the border of each ROI, excluding other ROIs, and subtracted this neuropil fluorescence from the ROI fluorescence, scaled by a correction factor: $F_{correct} = F_{ROI} - cf \times F_{neuropil}$. The correction factor accounts for the amount of contamination from the neuropil (Chen et al. 2013; Kerlin et al. 2010). To estimate the correction factor, we computed the ratio between the pixel intensity within a manually selected blood vessel and that of a neighboring neuropil region devoid of ROIs, subtracting from both an offset value given by the off-lens

fluorescence pixel intensity. The resulting correction factor ranged from 0.4 to 0.8.

To express the fluorescence time series as relative changes in fluorescence, we calculated the $\Delta F(t)/F_0(t)$ as $(F_{correct}(t) - F_0(t))/F_0(t)$ where $F_{correct}(t)$ is the neuropil-subtracted fluorescence trace for each ROI. Because we wished to look at the relatively long-term changes in fluorescence that occur with changes in brain state, there was no clear baseline period in this experimental design. Consequently, $F_0(t)$ was estimated as periods when the ROI was relatively inactive (Peters et al, 2014). We calculated the variance of $F_{correct}(t)$ for each ROI in 10-second bins and identified inactive epochs as the periods when the variance was below the 20th percentile. Values between the identified inactive periods were linearly interpolated to estimate the $F_0(t)$, which was then used to calculate the $\Delta F_{correct}/F_0(t)$.

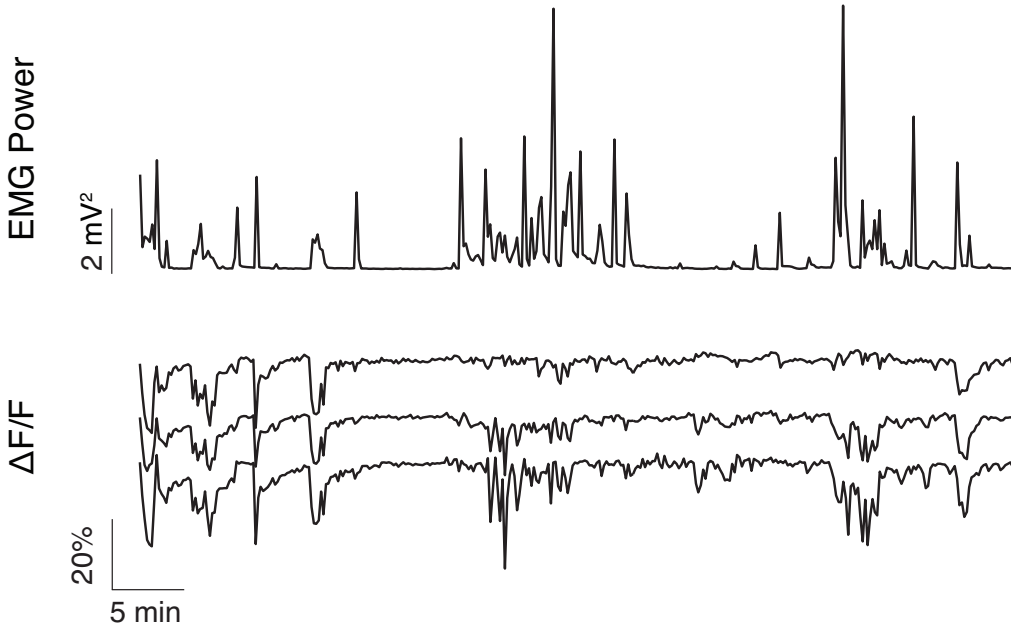

Figure 2.2. Motion artifact: EMG data and example ΔF/F traces from a GAD2-cre mouse expressing EYFP in GABAergic neurons. Increases in EMG activity are associated with negative deflections of the ΔF/F traces.

Imaging from the brainstem of unrestrained mice is accompanied by a fair amount of movement of the brain relative to the microendoscope. Although we can largely correct the lateral movements of the brain as described above, we cannot correct changes in fluorescence caused by the cells coming in and out of focus when the brain moves in the dorsal-ventral plane (Lovett-Barron et al. 2014). When we imaged from GAD2-cre mice injected with AAV2-syn-flex-EYFP (UNC Vector Core), most of the deflections in the fluorescence trace were negative (Figure 2.2). Consequently, a further correction to the $\Delta F_{correct}/F_0(t)$ was made by identifying negative deflections that had an amplitude at least two

standard deviations greater than the mean of the fluorescence trace. The corresponding frames were excluded from later analysis. Subsequently, $\Delta F_{correct}/F_0(t)$ will be referred to as ΔF/F.

The ΔF/F traces obtained with GCamp6s imaging did not resemble the EYFP data very closely. These negative transients, although present, are not as prominent in ROIs expressing GCaMP6s, suggesting that increases in fluorescence with movement may be masking the artifacts. Therefore, it is possible that the changes in fluorescence during wake are in fact underestimated.

Evaluation of brain state modulation: To determine the activity of each ROI across the sleep-wake cycle, the average ΔF/F was extracted during each state. Because we saw little activity during NREM, and found no ROIs that were maximally active during NREM, the brain state modulation of the ROIs was sometimes expressed as an index of REM activity relative to wake activity, calculated as the average ΔF/F activity during REM subtracted by the average ΔF/F activity during wake divided by their sum. This index gives an indication of how selective the ROI's activity is for periods of REM versus wake. An index of REM or wake relative to NREM activity was also calculated. Average ΔF/F during NREM was subtracted from the average ΔF/F activity during wake or REM sleep and then divided by their sum.

Classification of brain state modulation: ROIs were further categorized according to their pattern of activity across the three stages of the sleep-wake cycle. Significant brain-state modulation was assessed for each ROI using a one-way ANOVA, followed by unpaired t-tests or Wilcoxon rank-sum tests between all pairs of brain states, corrected for multiple comparisons using the Bonferroni method. Significantly modulated ROIs were then categorized as wake-max, REM-max or wake/REM active. None of the ROIs were maximally active during NREM sleep. An ROI was classified as wake-max if it was maximally active during wake and significantly more active during wake than during NREM and REM sleep ($p < 0.05$). An ROI was REM-max if it was maximally active during REM sleep and significantly more active during REM than NREM and wake ($p < 0.05$). Finally an ROI was classified as wake/REM active if its activity was not significantly different during REM and wake, but was significantly less active during NREM sleep ($p < 0.05$). A subset of the ROIs (3.7%) could not be classified according to these criteria, despite being significantly modulated by brain state (one-way ANOVA, $p < 0.05$).

Brain state transitions: To look at the temporal relationship between changes in neural activity and changes in global brain state, four types of transitions were identified from the EEG and EMG data: NREM to wake, REM to wake, wake to NREM and NREM to REM. For all transition types, except for wake to NREM, transitions which were preceded and followed by at least 20 seconds of the appropriate state, were averaged across all cells. To estimate the

time of the transition in the ΔF/F activity, we first calculated the Z-score of the entire ΔF/F trace and then calculated the mean and standard deviation of the period between 10 and 20 seconds before each transition. The time of each neural transition was calculated as the point when the activity surpassed two standard deviations above the mean of this baseline period. The average transition time was then calculated for each ROI. Because the change in activity around the wake to NREM transition is slower, a 40 second period was considered around these transitions. The baseline mean and standard deviation were calculated from the period between 30 and 40 seconds prior to the transition for each instance of the transition, and the time of the change in neural activity was calculated as the point when the ΔF/F activity fell 2 standard deviations below the baseline mean.

Spatial organization of ROIs: To assess whether there is any spatial organization of the sleep-wake activity, an index of REM versus wake activity, as described above, was plotted as a function of medial-lateral position or anterior-posterior position of each ROI. The anatomical coordinate of the ROI was estimated based on the localization of the lesion as described in section 2.4. The center of the lesion was assumed to be the center of the lens, and each ROI's anatomical coordinate was calculated relative to that position. Because the representation of ROIs was not uniform across the anteroposterior and mediolateral space, we also looked at the REM versus wake activity of the surrounding neuropil. The neuropil was segmented into 20 μm x 20 μm regions, excluding identified ROIs, and the ΔF/F time series were extracted for each segment. The index of REM activity versus wake activity was then calculated for each neuropil region and the anatomical location defined as the center of the neuropil segment. To assess the relationship between the neuropil activity and anatomical location, mediolateral and anteroposterior axes were binned into 50 μm segments across all animals.

General Statistical Analyses: A one-way repeated measures ANOVA was used to assess the brain state modulation across cells. Data sets were then tested for normality with the Lilliefors modification of the Kolmogorov-Smirnov test and comparisons between pairs of brain states were made with a paired t-test or Wilcoxon signed rank test as appropriate, with the Bonferroni correction for multiple comparisons. To test the modulation of individual cells by state, a one-way ANOVA was used. After testing for normality, brain states were compared with an unpaired t-test or Wilcoxon rank-sum test with the Bonferroni correction for multiple comparisons as appropriate. Unless otherwise stated, error bars are mean $\pm$ standard error of the mean (s.e.m.).

2.6 Technical considerations

Damage to brain tissue: Microendoscope imaging with a head-mountable microscope and genetically encoded calcium indicator allows us to target specific populations of neurons and monitor their activity in the freely moving mouse. This method overcomes the depth limitations of single- and two-photon microscopy through the use of an implanted GRIN lens, which relays the imaging field from the deep brain structure of interest (Ghosh et al. 2011; Helmchen and Denk 2005). The GRIN lens is large, however, and brain tissue above the imaging site is damaged by its insertion. For these experiments we used a 0.5 mm diameter lens, which mostly damaged portions of the cerebellum and superior colliculus, which are unlikely to interfere with the regulation of the sleep-wake cycle. After implantation, subjects showed no obvious gross motor impairments. This is in contrast to earlier iterations of the procedure using a 1 mm diameter lens, which required aspiration of the overlying tissue. In addition to a much lower survival rate, many of the mice had an abnormal gait after surgery, listing towards one side. Implantation of a smaller lens without aspiration prevented these complications.

Spatial resolution: The head-mountable microscope is a single-photon, epifluorescence microscope with a lateral resolution of about 1 μm and therefore lacks the optical sectioning capabilities of two-photon or confocal microscopy (www.inscopix.com). Therefore, although individual cells can be discerned, structural information discernible with other methods is unavailable with microendoscope imaging. The depth of field is also greater, so out of focus neurons and fibers above and below the ROI can contaminate the signal. Our neuropil subtraction protocol is detailed in section 2.5, but incomplete correction could, in principle, still effect our measurements. One concern is that neuropil contamination would lead to spurious correlations between ROIs' activity. To address this we computed the correlation between each ROI and all other ROIs in a given imaging field and compared this to the correlations between the surrounding neuropil regions that are used for the neuropil subtraction described above. The correlations between the neuropil regions were significantly higher than the correlations between ROIs ($R = 0.88 \pm 0.12$ for the neuropil and $R = 0.68 \pm .18$ for the ROIs, $p = 1.3 \times 10^{-20}$, Wilcoxon rank sum test). Correlation between the ROIs is not surprising given the slow, global nature of the brain state changes for which these neurons are important. However, it is not possible to ensure that the high correlations between ROIs are not due in part to contamination from the neuropil without simultaneous, cell-attached recordings. Despite the possibility of residual contamination, given that the GCaMP6s is specifically expressed in a single type of neuron for a given mouse, the neuropil signal is still specific to the neuronal subtype of interest. We will therefore, still be able to assess the activity of the GABAergic, glutamatergic and cholinergic populations across the sleep-wake cycle.

Temporal resolution: Finally, because microendoscope imaging does not allow for simultaneous, cell-attached recordings it is currently impossible to ascertain how calcium dynamics relate to the underlying action potentials. Boucetta et al reported instantaneous firing rates between 10 and 76 Hz for glutamatergic and GABAergic neurons in this region, which are well above the temporal resolution of the GCaMP6s indicator (Boucetta et al. 2014; Chen et al. 2013). This means that the calcium transients from multiple action potentials are likely merged to make up fluorescence events. Given that we were measuring changes in activity over long periods of time, corresponding to the slow dynamics of the sleep-wake cycle, this should not effect conclusions regarding the general pattern of activity for the different groups of cells. The high firing rate and slow dynamics of the calcium indicator will likely affect the amplitude of the recorded responses. Therefore, the activity profiles for different neuronal populations should still be discernible, but comparisons of the response amplitude between ROIs will be difficult. Furthermore, given the high firing rate of the GABAergic and glutamatergic neurons in this region it is possible that the calcium indicator could saturate. Saturation of the indicator could make it such that neurons that are modulated by brain state do not appear to be so: if a neuron has a very high firing rate across all brain states, further increases may not be detectible. This did not seem to affect our results too much as only 7 of the 161 imaged ROIs were not significantly modulated by brain state. It is also possible that the dynamics of the calcium indicator led to an underestimation of the brain state selectivity of a given ROI. If the neuron is highly active in two states, but still significantly more active in one, it is possible that saturation or sublinear summation of calcium transients could prevent the detection of this difference. This would result in an ROI being classified as equally active in the two states even though it is more selective for one of them. The merging of calcium transients from individual action potentials could also contribute to the high correlation between ROIs. If an ROI's activity is increasing generally during a given state, it is possible that temporally finer increases in activity may be masked.

Chapter 3: Brain state modulation of identified neurons in the laterodorsal tegmental nucleus

3.1 Preface

It is well established that acetylcholine (ACh) is important for the cortical activation (or desynchronization) that occurs both during active, attentive periods of wakefulness and during REM sleep. The laterodorsal tegmental nucleus (LDT) is one of the primary ACh-containing nuclei within the mesopontine tegmentum of the brainstem. Cholinergic neurons within the LDT are thought to effect cortical activity and sleep-wake behavior via projections to the basal forebrain, thalamus, brainstem reticular formation and descending projections to other brainstem nuclei. (Jones 2008; Paré et al. 1988; Semba et al. 1990) Furthermore, previous electrophysiology experiments have found these cholinergic neurons to be most active during periods of wake and REM sleep. This nucleus is comprised of multiple, intermingled cell types, however, and it is less clear how their activity is modulated across the sleep-wake cycle (Clements & Grant 1990; Ford et al. 1995; Wang & Morales 2009).

Although early pharmacology studies led to the hypothesis that REM sleep induction was primarily mediated by the interaction between cholinergic and monoaminergic systems in the brainstem, the importance of pontine glutamatergic and GABAergic signaling for REM sleep has been demonstrated as well (Lai & Siegel 1988; Lu et al. 2006; Luppi et al. 2006; Nitz & Siegel 1997). Thus, further evaluation of the brain state related activity of non-cholinergic LDT neurons will help clarify the brainstem circuitry mediating sleep-wake behavior.

In order to characterize the brain state-specific activity of identified neurons in this region, we transfected GABAergic, glutamatergic or cholinergic neurons located within the LDT with the calcium indicator GCaMP6s. We then imaged their activity using a microendoscope and head mountable fluorescence microscope in the freely moving mouse as it transitioned naturally through the sleep-wake cycle. These experiments further allowed us to determine whether the glutamatergic and GABAergic neurons form heterogenous groups, in which case, microendoscope imaging permits us to assess the spatial relationship between different neurons, to determine whether there is any anatomical organization of response properties within the LDT.

3.2 Imaging brain state dependent activity in the brainstem

To target different subtypes of neurons in the LDT, GAD2-IRES-cre, Vglut2-IRES-cre or ChAT-IRES-cre mice were injected with AAV1-syn-flex-

GCaMP6s to allow for cell-type specific expression of the GCaMP6s calcium indicator in GABAergic, glutamatergic or cholinergic neurons respectively (Chen et al. 2013). The mice were then implanted with a microendoscope over the injection site as well as cortical EEG and neck muscle EMG electrodes to allow for simultaneous calcium imaging and monitoring of ongoing brain state as the mouse slept freely in its home cage. The LDT is located in the mesopontine tegmentum, deep in the brain, so to image from this structure, we used a gradient refractive index (GRIN) lens, which relays the image from the brainstem to a focal plane outside of the brain, which can then be acquired with a miniaturized, head mountable microscope (Figure 3.1a)(Ghosh et al. 2011). The mouse is able to move freely in its cage while the microscope is affixed to its skull. This technique allowed us to simultaneously monitor the activity of multiple, identified neurons in the LDT to assess how their activity varied with brain state.

Figure 3.1b shows an example imaging field from a GAD2-IRES-cre mouse in which multiple neurons expressing GCaMP6s could be identified. These regions of interest (ROIs) are outlined in the second panel. Relative fluorescence changes from a subset of these ROIs across epochs of wake, NREM sleep and REM sleep are shown in Figure 3.1c, along with simultaneously

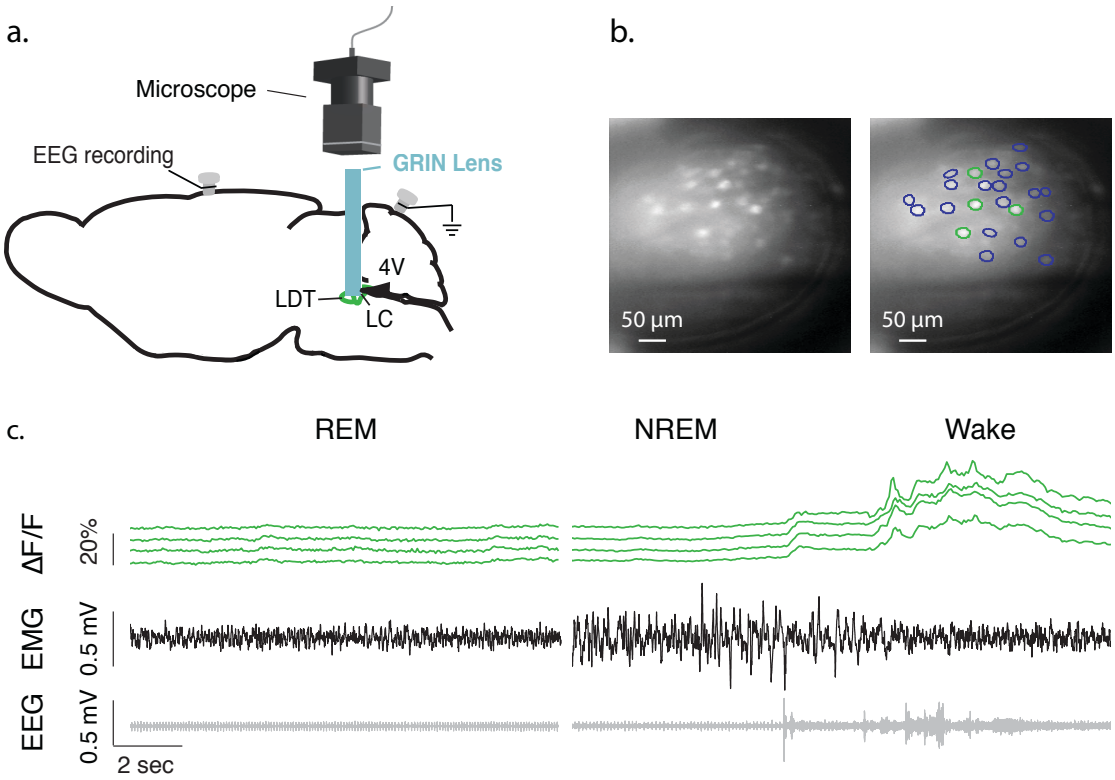

Figure 3.1 a) Schematic of experimental setup **b)** An example imaging field from a GAD2-cre mouse with multiple outlined ROIs. **c)** Example ΔF/F traces (ROIs circled in green in **b**), EEG and EMG traces during periods of REM, NREM and wake. LDT: laterodorsal tegmental nucleus; LC: locus coeruleus; 4V: fourth ventricle

acquired EEG and EMG data. These GABAergic ROIs show very little fluctuation in fluorescence during REM sleep or NREM sleep. The fluorescence increases markedly when the mouse transitions into wake, however, and the EMG activity increases while the high-amplitude, low-frequency EEG activity decreases, in favor of high frequency low amplitude EEG. This suggests that these GABAergic neurons are wake active.

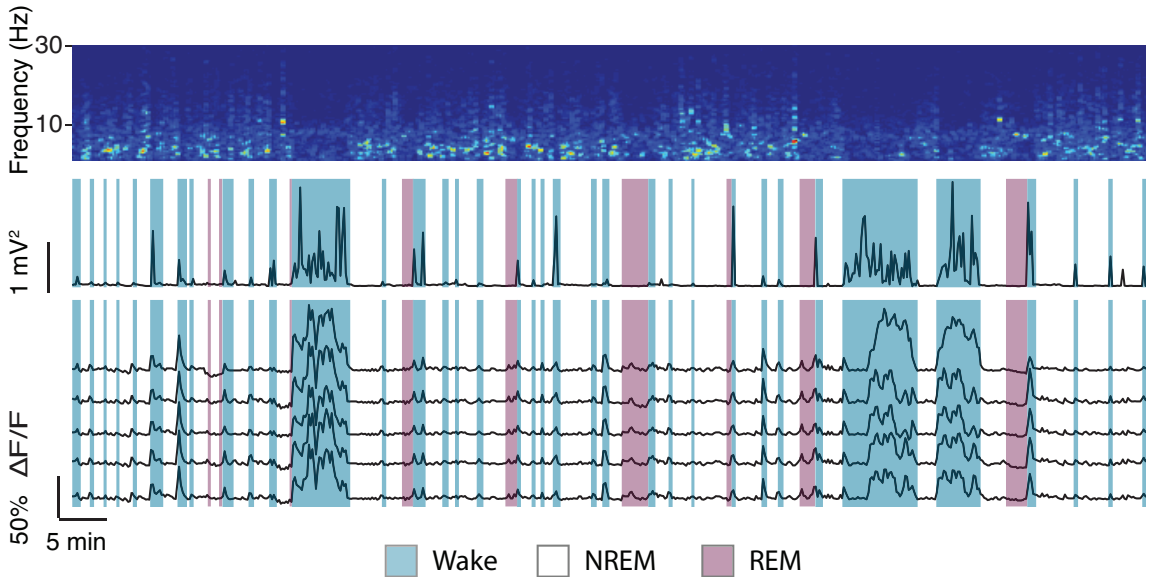

Figure 3.2: Modulation of GABAergic activity across the sleep-wake cycle. The top panel shows the frequency decomposition of cortical EEG. The second panel is the EMG power, which is used in combination with the EEG to classify the animal's brain state. The classified brain state is indicated by the color code.The bottom panel shows the ΔF/F traces from several simultaneously imaged ROIs in a GAD2-IRES-cre mouse.

3.3 Brain state modulation of GABAergic neurons in the LDT.

We imaged the activity of 105 putative GABAergic neurons from 6 adult mice across the sleep-wake cycle. Figure 3.2 shows the calcium dynamics of several simultaneously imaged ROIs from a GAD2-IRES-cre mouse across periods of wake, NREM and REM sleep. When the mouse was awake, especially during active periods indicated by high EMG power, there was a pronounced increase in activity compared to all stages of sleep.

The population of GABAergic neurons was significantly modulated by state, (one-way repeated measures ANOVA, $p = 4.4\text{x}10^{-30}$, $n = 105$) and were more active during periods of wake compared to NREM and REM sleep (Wilcoxon signed-rank test with Bonferroni correction for multiple comparisons $p = 5.8\text{x}10^{-19}$ and $1.2\text{x}10^{-12}$ respectively; Figure 3.3).

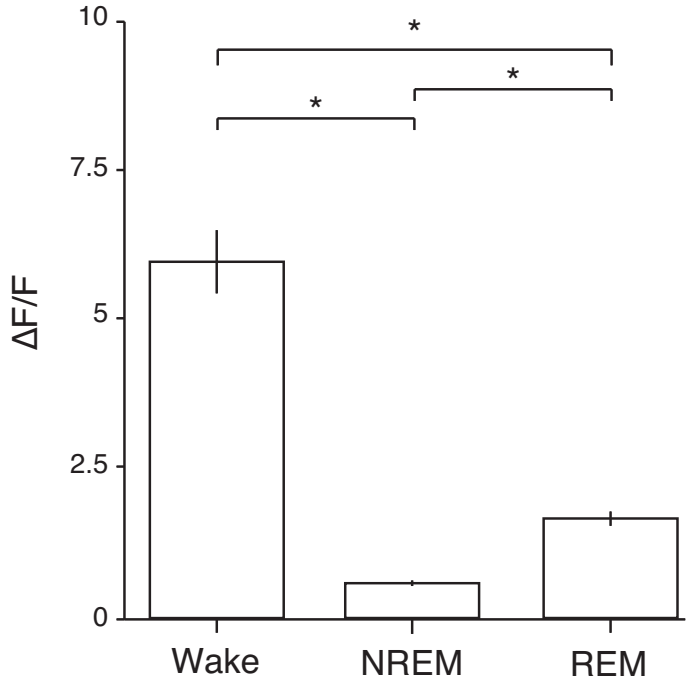

Figure 3.3: Average activity of GABAergic neurons across the sleep-wake cycle. The ΔF/F activity in each state is averaged across all ROIs. * $p < 1.2x10^{-12}$ Wilcoxon signed rank test

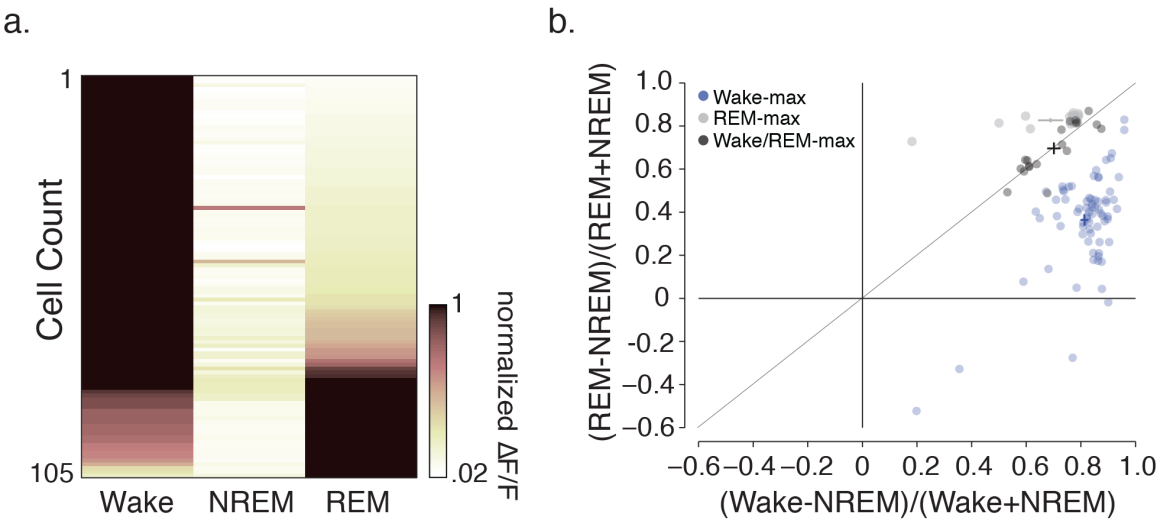

Figure 3.4 Brain state modulation of GABAergic ROIs. a) Each ROI's activity during wake, NREM and REM is normalized to its maximally active state and plotted such that each row corresponds to one ROI's average activity in each identified brain state. **b**) ROIs are plotted as an index of wake activity relative to NREM activity versus an index of REM activity relative to NREM activity. Each ROI has been categorized as wake-max (blue), REM-max (gray) or wake/REM active (black). The mean and standard error of the mean is plotted for each group.

Individually, all of the imaged GABAergic ROIs were significantly modulated by brain state as well (one-way ANOVA, $p < .001$). Figure 3.4a shows the average activity of each cell during wake, NREM and REM normalized to its maximally active state. Although the neurons do not have completely uniform responses, the majority are maximally active during wake (81/105), with a smaller group most active during REM sleep (24/105). None of the imaged GABAergic ROIs were maximally active during NREM sleep. To evaluate how the strength and specificity of brain state modulation varies across the population of GABAergic neurons, we plotted each ROI's wake activity relative to NREM activity versus its REM activity relative to NREM activity (calculated as the difference between wake or REM activity and NREM activity divided by their sum). Most of the ROIs are positioned in the upper right quadrant, indicating greatest activity during REM and wake. Not only does the degree of REM or wake modulation vary in amplitude, but the specificity of a given ROI's REM and wake response varies as well. Most of the cells show greater wake-related activity modulation, but a subset are more active during REM sleep and a number of ROIs have roughly equal modulation along the REM and wake axes.

Given the heterogeneity of the GABAergic responses, we next divided the ROIs into three categories according to their pattern of activity across the three states. ROIs were categorized as wake-max, REM-max or wake/REM-active. Wake-max ROIs had significantly higher $\Delta F/F$ activity during periods of wake than during REM and NREM (Wilcoxon rank sum test, $p < 0.01$, $n = 72$). This was the largest subset of significantly modulated GABAergic ROIs (68.57%), followed by wake/REM-active (18.10%) and REM-max (13.33%) ROIs. REM-max ROIs were most active during REM sleep and significantly more active during REM than NREM and wake (Wilcoxon rank sum test, $p < 0.01$, $n = 14$). Finally, the wake and REM activity of wake/REM ROIs was not significantly different, but activity during each was significantly greater than during NREM sleep (Wilcoxon rank sum test, $p < 0.01$, $n = 19$). The points are color coded according to this categorization in Figure 3.4b and the average wake modulation versus REM modulation is shown for each group.

We next looked at whether the changes in GABAergic LDT activity preceded changes in global brain state. Figure 3.5 shows the average activity of all GABAergic ROIs around various state transitions. The animals' transitions into wake from either NREM or REM were anticipated by increases in GABAergic activity by 4.39 ± 0.16 seconds and 6.30 ± 0.24 seconds (mean $\pm$ standard error of the mean) respectively. The distributions of the latencies across ROIs, which were significantly different from zero (Wilcoxon sign rank test, $p = 5.83 \times 10^{-19}$ and $p = 5.82 \times 10^{-19}$), are plotted in the insets. Indicative of the higher amount of REM activity than NREM activity, the average $\Delta F/F$ in the REM period preceding the transition into wake is significantly higher than the NREM period preceding the transition into wake (Wilcoxon sign rank test, $p = 2.2 \times 10^{-14}$). The transition from NREM to REM is also accompanied by an anticipatory increase in GABAergic activity (4.5 ± 0.23 sec, paired t-test $p = 1.04 \times 10^{-18}$) and GABAergic fluorescence decreases prior to the transition into NREM sleep from wake. This transition is

more gradual than the others, perhaps due to the slow progression through quiet wake into sleep, and individual ROIs show a much greater variation in the onset of their decrease in activity around this type of transition compared to the others (5.58 ± 0.65 sec before the state transition, $p = 4.68 \times 10^{-11}$).

In contrast to the cholinergic neurons of the LDT (Boucetta et al. 2014; Jones 2008; Sakai 2012), we found the GABAergic neurons of this nucleus to be predominantly active during wakefulness. The population is not homogenous, however, and many neurons showed increases in activity during REM sleep as well. Furthermore, the activity of LDT neurons anticipated brain state transitions in and out of REM and wake states, allowing for the possibility that these neurons play a causal role in the pontine circuitry initiating and maintaining REM sleep and wake.

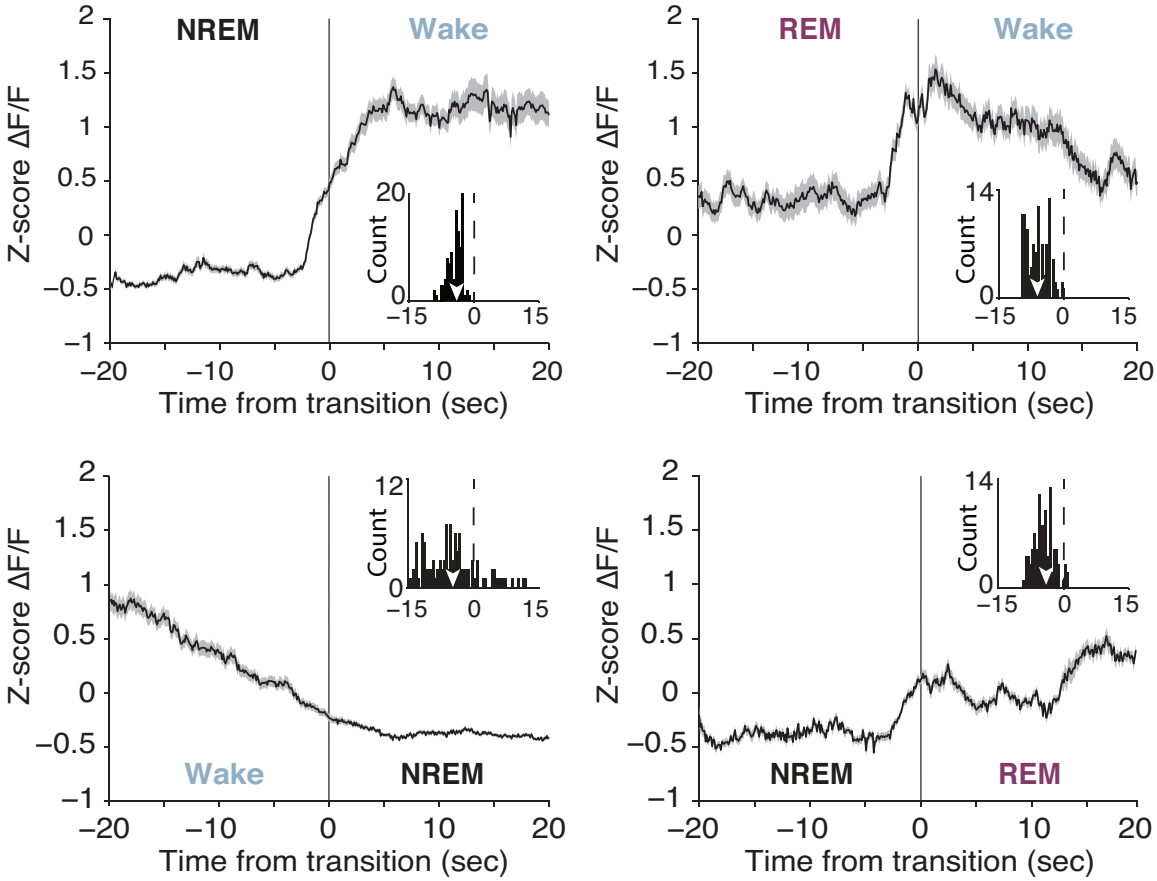

Figure 3.5: Changes in GABAergic activity precede brain state transitions. Each plot shows the transition triggered average of the Z-scored ΔF/F activity across all ROIs. Time zero is the time of brain state transition identified according to the EEG and EMG activity. The changes in fluorescence precede the brain state transition from NREM to wake, REM to wake, wake to NREM and NREM to REM. The insets show the distribution of the onset of the change in calcium activity relative to the brain state transition for all ROIs.

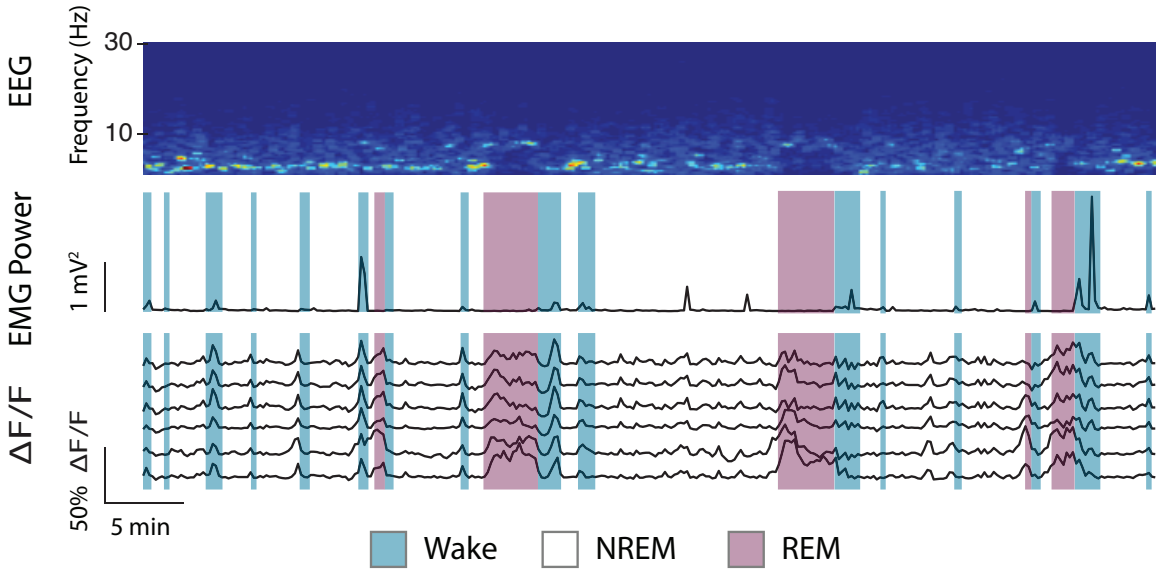

Figure 3.6: Modulation of glutamatergic activity across the sleep-wake cycle. The top panel shows the frequency decomposition of cortical EEG. The second panel is the EMG power, which is used in combination with the EEG to classify the animal's brain state, which is indicated by the color code. The bottom panel shows the ΔF/F traces from several simultaneously imaged ROIs.

3.4 Brain state modulation of glutamatergic neurons in the LDT

The other main population of non-cholinergic neurons in the LDT is comprised of glutamatergic neurons (Wang & Morales 2009). To assess their activity across the sleep-wake cycle, we injected AAV1-syn-flex-GCaMP6s into the LDT region of Vglut2-IRES-cre mice and imaged 52 neurons from 5 adult mice as above. Figure 3.6 shows an example imaging session of multiple glutamatergic ROIs as the mouse transitioned between sleep and wake. These glutamatergic ROIs show increased activity not only during periods of wake, but during REM sleep as well. The population of glutamatergic neurons was significantly modulated by state (one-way, repeated measures ANOVA, $p = 5.8 \times 10^{-9}$, Figure 3.7). Unlike the GABAergic neurons, which predominantly showed increased activity during wake, the glutamatergic ROIs were on average significantly more active during REM sleep than during NREM and wake (Wilcoxon signed rank test with Bonferroni correction for multiple comparisons, $p = 1.0 \times 10^{-9}$ and $p = 2 \times 10^{-4}$ respectively, Figure 3.7). In Figure 3.8a, the activity in each of the three states is normalized to the maximally active state and plotted for every ROI. Most of the glutamatergic ROIs were most active during REM sleep (67.3%) and the rest were most active during wake (48.6%). None of the imaged glutamatergic ROIs were most active during NREM.

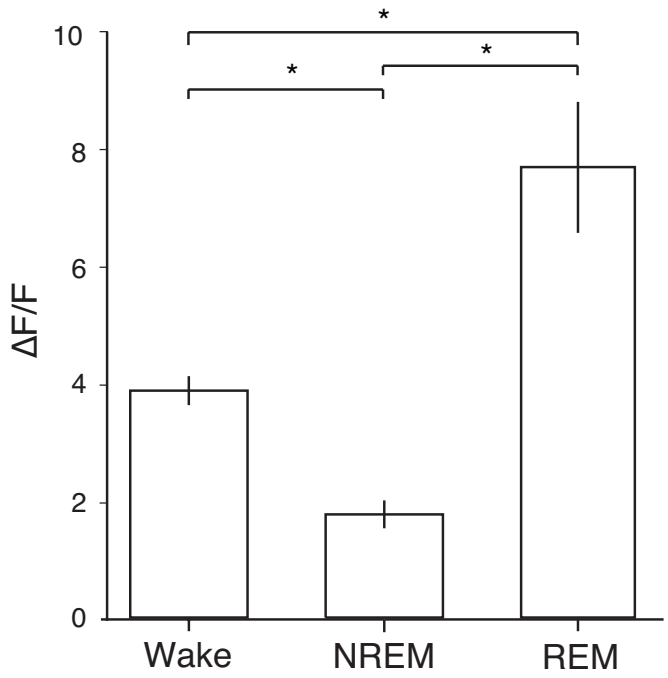

Figure 3.7: Average activity of glutamatergic neurons across the sleep-wake cycle The ΔF/F activity in each state is averaged across all ROIs. * $p < 1.0x10^{-9}$ Wilcoxon signed rank test

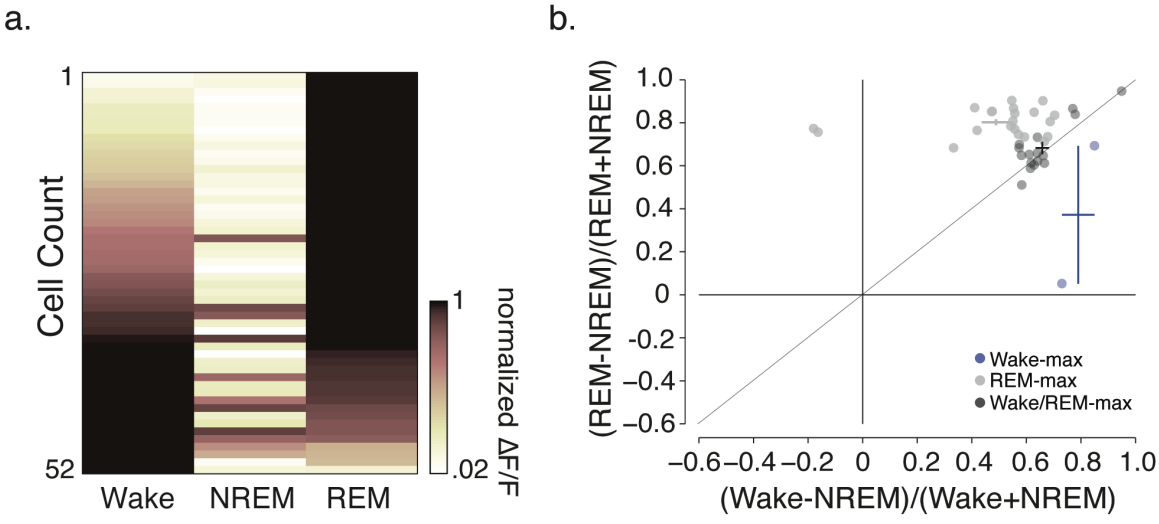

Figure 3.8: Heterogeneity of brain state modulation of glutamatergic ROIs. a) Each ROI's activity during wake, NREM and REM is normalized to its maximally active state and plotted such that each row corresponds to one ROI's activity. **b)** The significantly modulated ROIs are plotted as an index of wake activity relative to NREM activity versus an index of REM activity relative to NREM activity. Each ROI has been categorized as wake-max (blue), REM-max (gray) or wake/REM max (black).

Forty-five of the 52 imaged glutamatergic ROIs were significantly modulated by state (one-way ANOVA, $p < 0.05$). Like the GABAergic cells, the significantly modulated glutamatergic ROIs could be classified according to their pattern of activity across the sleep-wake cycle. The largest subgroup of glutamatergic ROIs were significantly more active during REM sleep than NREM and wake (REM-max, 46.67%), followed by the wake/REM active ROIs (35.6%). Only 4.4% were wake-max ROIs and 13.3% were undefined. Although the undefined ROIs were significantly modulated by brain state (one-way ANOVA, $p < 0.05$), the activity of these ROIs could not be classified according to the *post-hoc* pairwise tests. Figure 3.8b shows the activity of each significantly modulated

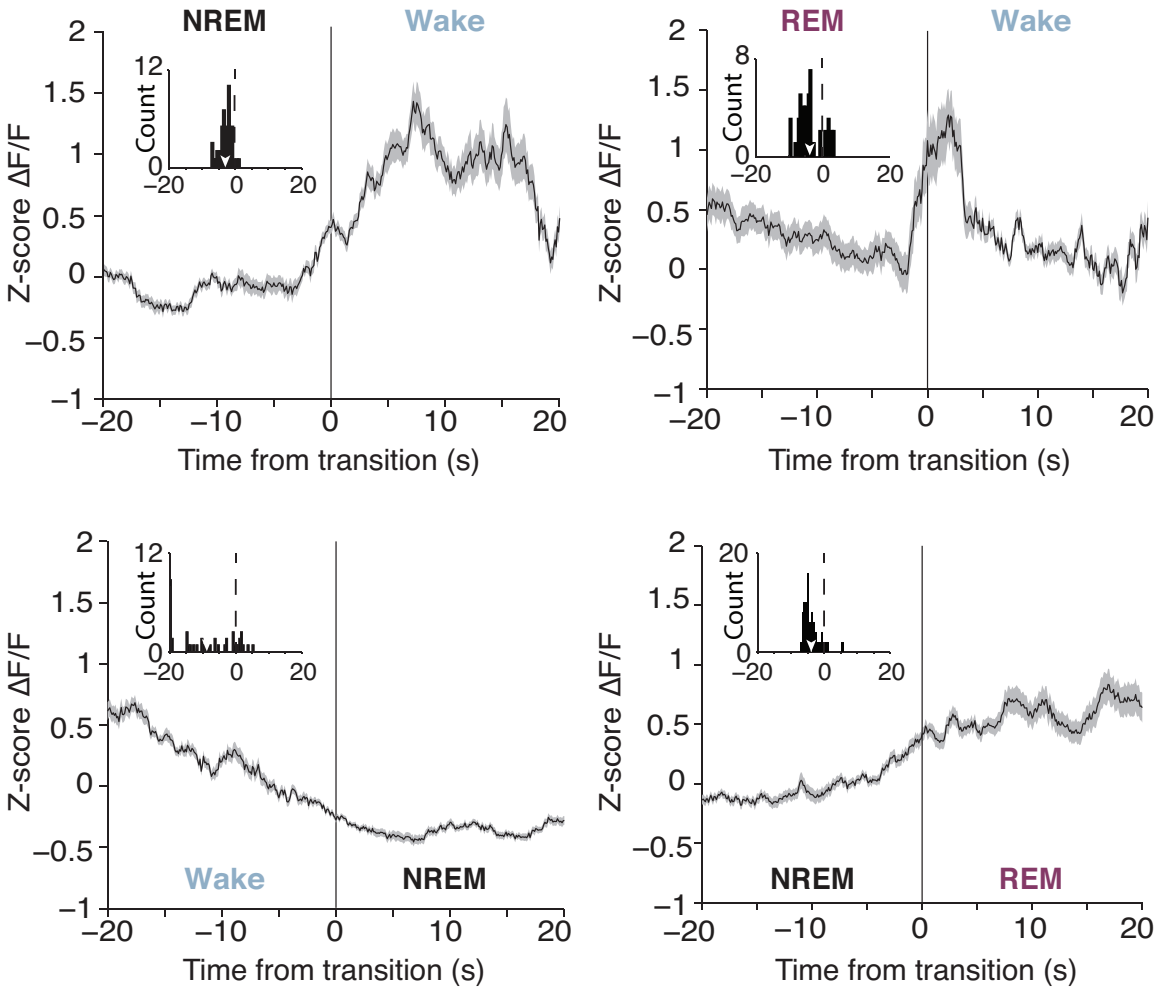

Figure 3.9: Changes in glutamatergic activity precede brain state transitions. Each plot shows the transition triggered average of the Z-scored ΔF/F activity across all ROIs. Time zero is the time of brain state transition identified according to the EEG and EMG activity. The changes in fluorescence precede the brain state transition from NREM to wake, REM to wake, wake to NREM and NREM to REM. The insets show the distribution of the onset of the change in calcium activity relative to the brain state transition for all ROIs.

and classifiable glutamatergic ROI as an index of wake modulation versus an index of REM modulation, and is color-coded according to category. Again we can see that most of the brain state modulation of ROI activity is evident during wake and REM, but unlike the GABAergic ROIs, most of the glutamatergic ROIs are more active in REM sleep than in wake periods.

Similarly to the GABAergic cells, the change in glutamatergic activity preceded brain state transitions (Figure 3.9), although with shorter latencies. On average, glutamatergic ROIs started to increase their activity significantly before the transition from NREM to wake (2.72 $\pm$ 0.28 second, $p = 6.2\text{x}10^{-9}$, Wilcoxon sign rank test). Their activity increased 3.19 $\pm$ 0.46 seconds before the transition from REM into wake ($p = 1.3\text{x}10^{-7}$, Wilcoxon sign rank test) and 4.44 $\pm$ 0.34 seconds before the transition from NREM into REM ($p = 5.6\text{x}10^{-9}$, Wilcoxon sign rank test). Finally, the activity of the glutamatergic neurons decreases 7.53 $\pm$ 1.38 seconds before the transition from wake into NREM sleep ($p = 1.3\text{x}10^{-5}$,Wilcoxon sign rank test). The changes in glutamatergic activity preceding transitions into wake occur significantly later than the GABAergic transitions ($p = 5.9\text{x}10^{-7}$ for NREM to wake transitions and $p = 6.2\text{x}10^{-8}$ for transitions from REM to wake, Wilcoxon rank sum test). This suggests that the putative wake-promoting actions of the GABAergic LDT neurons initiate before the activation of the glutamatergic neurons.

3.5 Brain state modulation of cholinergic neurons in the LDT

Although the involvement of brainstem cholinergic neurons in the regulation of REM sleep and wake has been well studied, and the modulation of individual neurons by ongoing brain state assessed (Boucetta et al. 2014; Sakai 2012; Yamamoto et al. 1990; Siegel 2013), microendoscope calcium imaging with a genetically encoded calcium indicator provides an opportunity to identify cholinergic neurons *in vivo* and to monitor the activity of multiple neurons at once. The activation pattern of imaged cholinergic neurons agrees with previous studies, showing increased fluorescence during both periods of wake and REM sleep (Figure 3.10 and 3.11a). The activity of the cholinergic ROIs was significantly modulated by state (one way, repeated measures ANOVA, $p = 0.009$) and activity during wake and REM was significantly greater than NREM (paired t-test, $p = 0.036$ and $p = 0.034$ respectively) but were not significantly different from each other (paired t-test, $p = 0.464$). All imaged cholinergic ROIs (n=4) were significantly modulated by state (one-way ANOVA, $p < .001$). Three were classified as wake/REM active while one was classified as REM-max (Figure 3.11b).

3.6 Spatial organization of LDT sleep-wake activity.

Microendoscope imaging gives us the opportunity not only to monitor the activity of multiple neurons at once, but also to identify their spatial relationship. Because we saw some heterogeneity in the sleep-wake activity of LDT neurons,

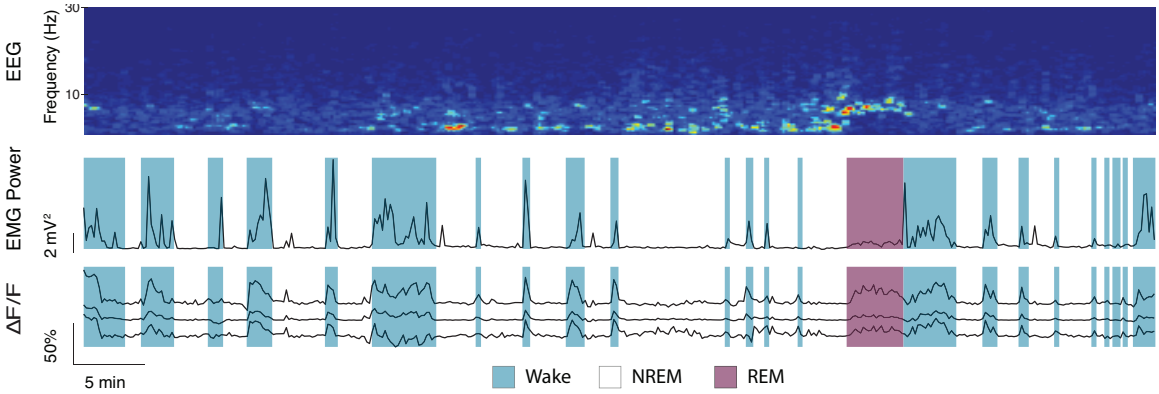

Figure 3.10: Modulation of cholinergic activity across the sleep-wake cycle. The top panel shows the frequency decomposition of cortical EEG. The second panel is the EMG power which is used in combination with the EEG to classify the animal's brain state which is indicated by the color code. The bottom panel shows the ΔF/F traces from several simultaneously imaged ROIs.

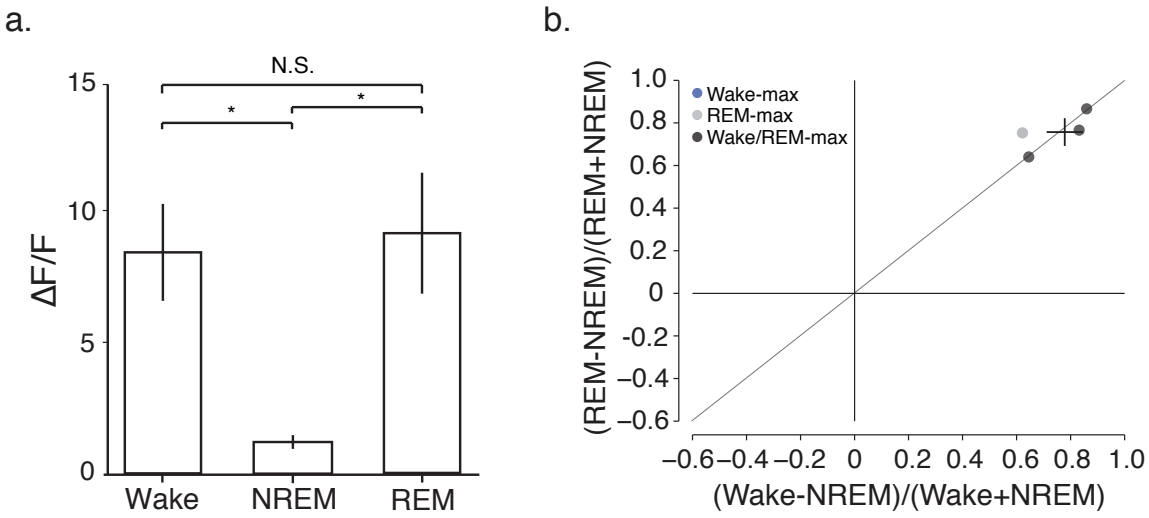

3.11 Average activity of cholinergic neurons across the sleep-wake cycle. a) Average brain state activity averaged across all cholinergic ROIs **b)** Wake modulation versus REM modulation relative to NREM activity of all cholinergic ROIs divided by category. N.S. not significant; * $p < 0.036$

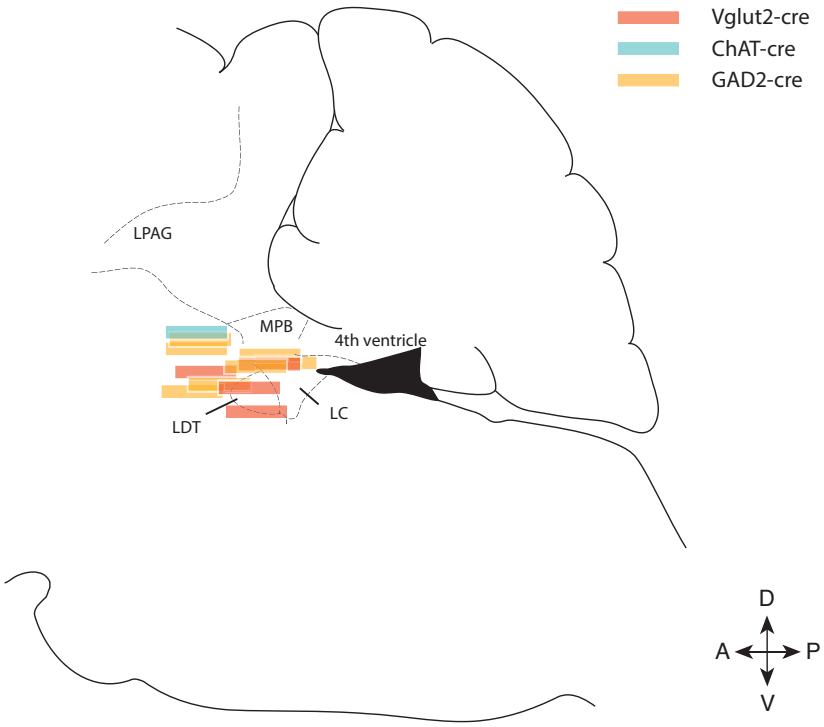

Figure 3.12: Imaging sites. The position of each lesion is marked and color-coded according to cell type, showing the full anteroposterior extent of the lens.

we next assessed whether there was any spatial organization of ROI sleep-wake responses. The imaging sites were distributed throughout the LDT, from approximately 4.7 mm to 5.8 mm posterior from bregma and mediolaterally from approximately 0.2 to 0.9 mm from the midline (Figure 3.12) ROI position was estimated based on histological identification of the center of the lesion, relying on anatomical landmarks as well as either ChAT or TH immunostaining to identify the position of the PPT and LDT or the LC respectively.

Glutamatergic ROIs showed variation in the amount of REM selectivity in their sleep-wake activity patterns. Although many of the glutamatergic neurons were active during both REM and wake, a subset were primarily active in one state or the other. Figure 3.13a shows the REM versus wake activity of all glutamatergic ROIs plotted according to their estimated mediolateral and anteroposterior position. In Figure 3.13a it is possible to see some spatial organization of the REM selectivity of the glutamatergic ROIs. ROIs positioned more medially show higher REM activity relative to wake activity compared to the more lateral ROIs. In Figure 3.13b the REM-Wake index is plotted as a function of the distance from the midline in the top plot and the distance from bregma in the bottom plot. The REM selectivity is highest in the ROIs positioned between about 0.2 and 0.4 mm from the midline, and quickly the levels of REM and wake activity become about even, as the index falls to zero at more lateral sites. Although the representation of glutamatergic ROIs is somewhat sparse, the anteroposterior organization of these ROIs suggests that both the most anterior

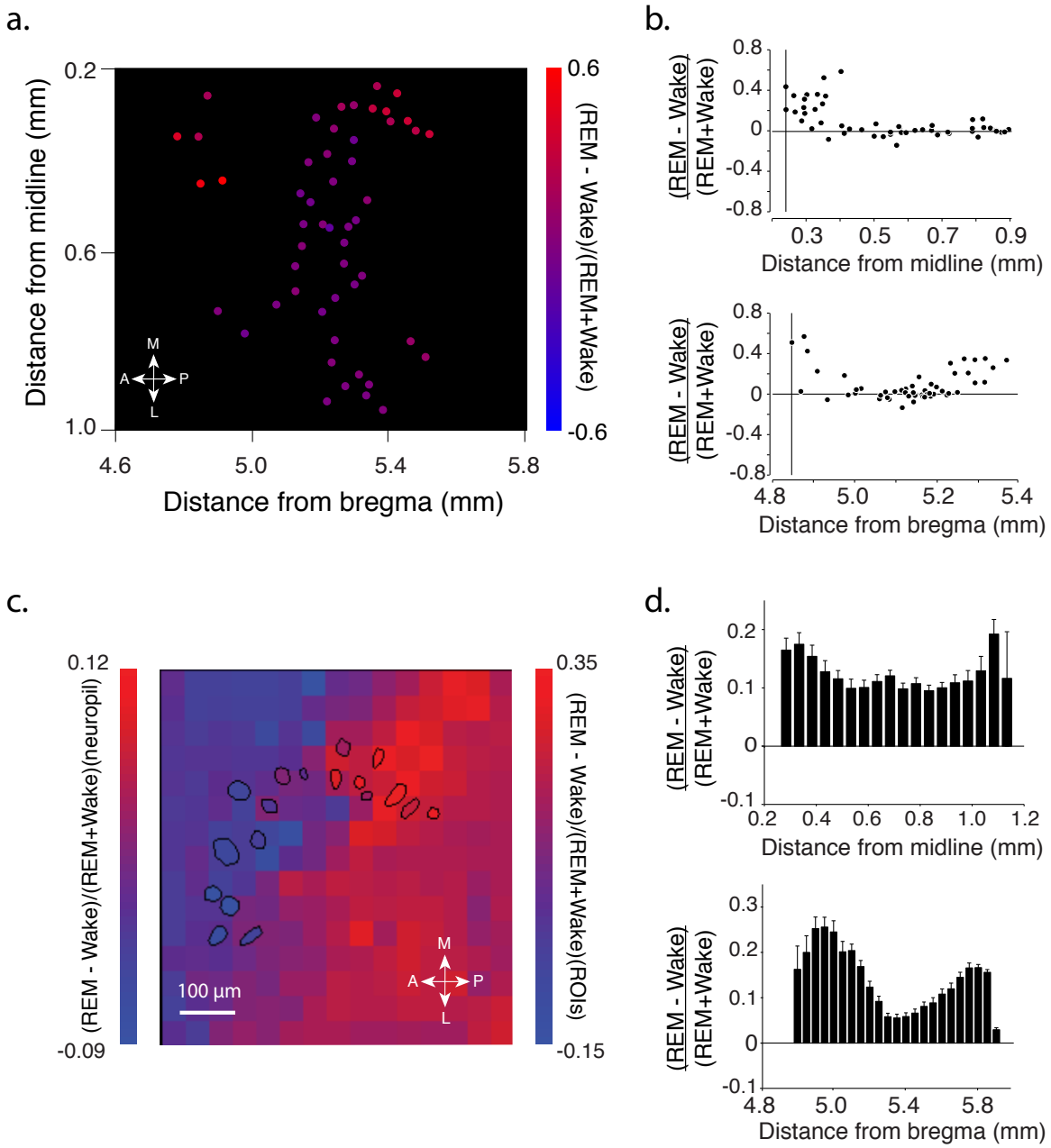

Figure 3.13: Spatial organization of glutamatergic REM and wake activity. a) REM versus wake activity of glutamatergic ROIs plotted according to anatomical coordinates. **b)** REM versus wake index as a function of the distance from the midline and bregma. **c)** Example distribution of neuropil REM versus wake activity. **d)** Spatial distribution of neuropil REM versus wake activity

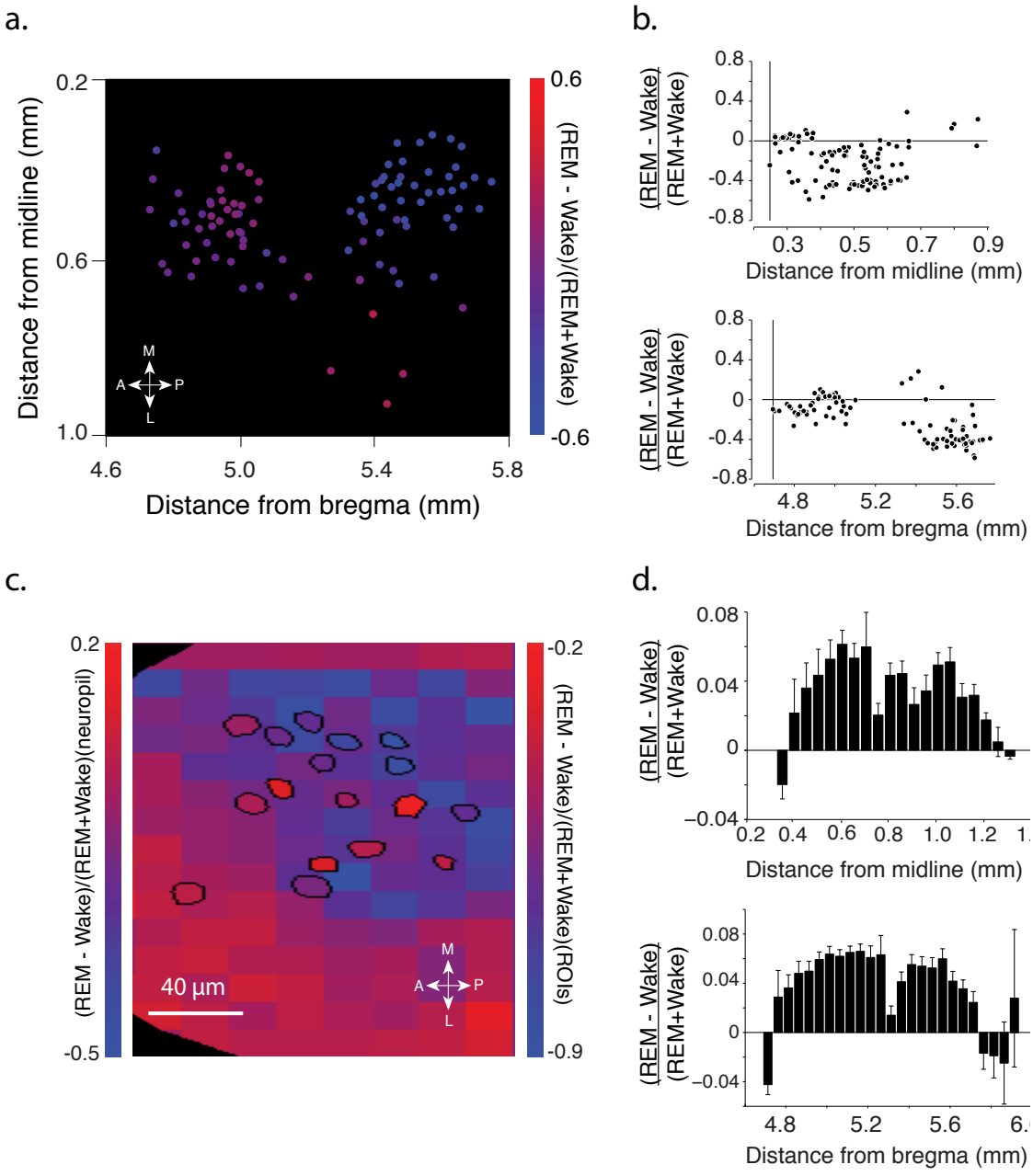

Figure 3.14: Spatial organization of GABAergic REM and wake activity. a) REM versus wake activity of GABAergic ROIs plotted according to anatomical coordinates. **b)** REM versus wake index as a function of the distance from the midline and bregma. **c)** Example distribution of neuropil REM versus wake activity. **d)** Spatial distribution of neuropil REM versus wake activity

and the most posterior portions of this pontine region contain neurons that are more selectively REM active. Because the ROIs did not uniformly tile the imaged area, we also looked at the brain-state related activity of the neuropil in each animal. Figure 3.13c shows the REM versus wake activity across the imaging field from an example Vglut2-IRES-cre mouse. The ROIs as well as the surrounding neuropil are color coded according to REM-wake index; the redder regions are more REM selective while the blue are more wake-selective. The brain state modulation of the neuropil activity shows a similar gradient to the ROIs, with increased REM selectivity in the medial and posterior regions. If we combine the neuropil activity across all animals in 50 µm bins (Figure 3.13d), there is a significant relationship between the REM-wake index and anatomical position along both the anteroposterior and mediolateral axes (one-way ANOVA, $p = 0.003$ for mediolateral organization and $p = 3.33 \times 10^{-64}$ for anteroposterior organization). We repeated this analysis for the ROIs as well, which revealed a significant relationship between both anteroposterior and mediolateral position

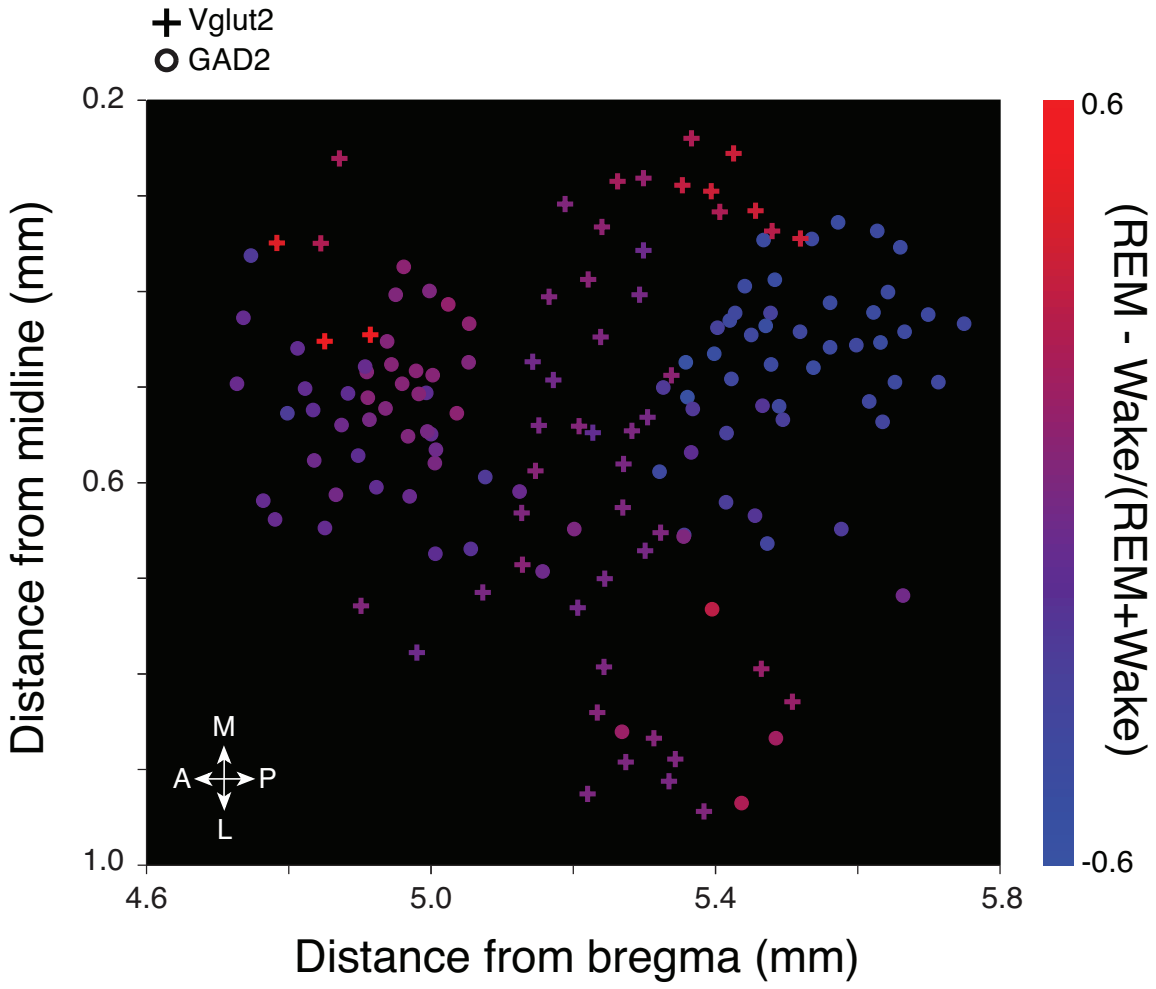

Figure 3.15: Spatial organization of glutamatergic and GABAergic LDT neurons

and REM-wake index (one-way ANOVA, $p = 0.007$ for mediolateral organization and $p = 5.48 \times 10^{-5}$ for anteroposterior).

The GABAergic neurons also vary in the amount of selectivity of their brain-state-related responses. Many of the ROIs have increased fluorescence during both wake and REM, but the more posterior ROIs are more wake selective than the more anterior ROIs. The mediolateral distribution of GABAergic activity is fairly uniform (Figure 3.14b), but the selectivity of the responses clusters into two groups when plotted along the anteroposterior axis. Most of these posterior ROIs are more wake-selective in their responses, but a small, more lateral cluster in this posterior region shows increased REM selectivity. The modulation of GABAergic neuropil activity is smaller than in the Vglut2-cre mice, but there is still a significant relationship between anatomical location and the REM-wake index (one-way ANOVA, $p = 0.002$ for mediolateral organization and $p = 1.59 \times 10^{-16}$ for anteroposterior organization). The relationship between activity and position is also significant for the ROIs along both the anteroposterior (one-way ANOVA, $p = 4.77 \times 10^{-11}$) and mediolateral (one-way ANOVA, $p = 4.03 \times 10^{-6}$) axes.

It seems that the more posterior and medial portions of this LDT region contain more state-specific neurons, with the GABAergic ROIs more selectively active during wake and the glutamatergic ROIs more selectively active during REM. Figure 3.15 shows all glutamatergic and GABAergic ROIs plotted in the same anatomical space, where the overlap of REM or wake selectivity is evident in the more posterior and medial locations.

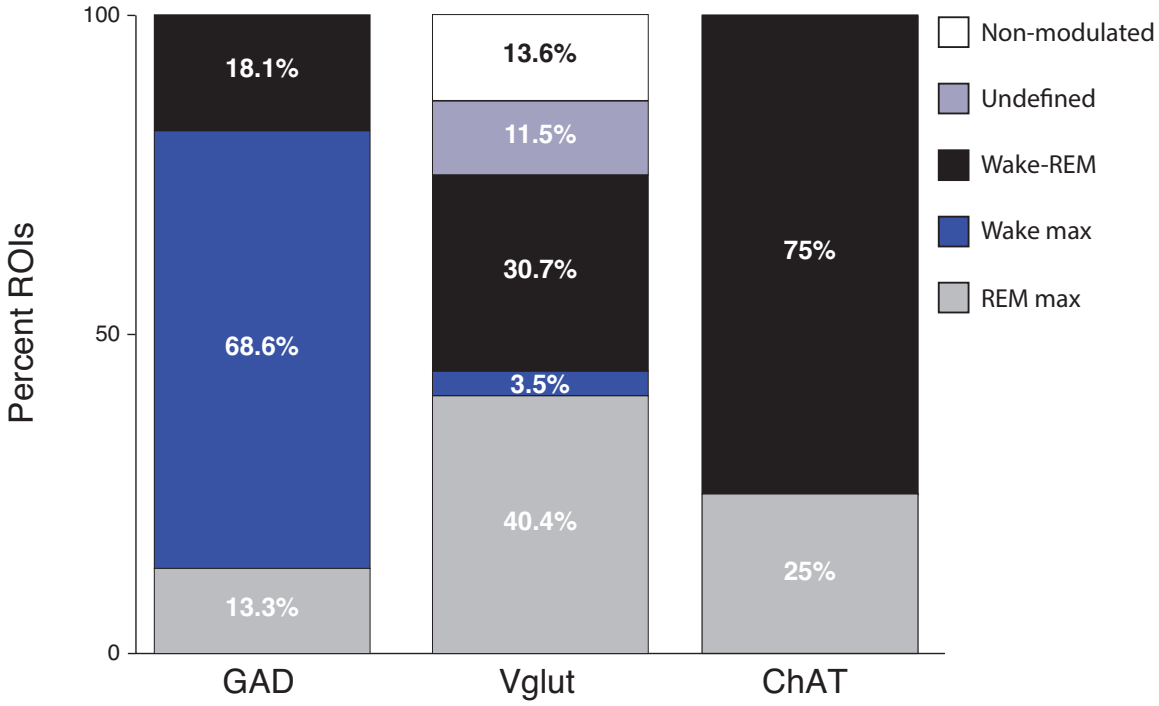

3.16: Composition of LDT neuronal subgroups. Shows the proportion of GABAergic, glutamatergic and cholinergic neurons in each sleep-wake category.

The spatial organization of glutamatergic and GABAergic brain-state-selective activity suggests that the behavioral effect of manipulating these neurons will be location dependent. Stimulating GABAergic neurons in the more posterior region may promote wakefulness, or even selectively suppress REM if these inhibitory neurons make synaptic contacts with the neighboring REM-active glutamatergic neurons. It is also possible that the neurons in the different regions of the LDT are involved in different features of REM sleep. Those that are active during both REM and wake (the purple ROIs in figures 3.13-3.15) could be involved in the modulation of cortical desynchronization, a property shared by both REM and wake. In contrast, the more REM selective ROIs may be involved in a REM specific feature such as muscle atonia.

In general, the neurons of the LDT region increase their activity during REM sleep and wakefulness and remain quiet during NREM sleep. Although each of the examined neuronal populations follows this general pattern, there is variation in the selectivity of and preference for REM or wake activity in the different groups. Except for the population of cholinergic neurons, which did not contain any wake-max ROIs, each neuronal class included the same sleep-wake activity profiles, but in different proportions. The number of imaged cholinergic neurons is very small, so it is possible that with more extensive sampling different patterns of activity would emerge as well. In this study, the GABAergic cells were dominated by maximally wake active neurons while the glutamatergic cells were primarily maximally active during REM or both wake and REM (Figure 3.16). The patterns of activity we found in the LDT region broadly agree with previous electrophysiological studies. Sakai recorded from the LDT region of unanesthetized, head-restrained mice and found both cholinergic and non-cholinergic neurons that were active during REM and wake along with non-cholinergic (and non-noradrenergic) neurons that were wake active (Sakai 2012). Only a subset of the cholinergic and noradrenergic neurons were histochemically identified in that study, however, and the identity of many of the wake-active and Wake/REM active cells were unknown. Using juxtacellular recording and immunohistochemistry, Boucetta and colleagues recently recorded the activity of glutamatergic, GABAergic and cholinergic neurons in the LDT region of the head-restrained rat (Boucetta et al. 2014). They found glutamatergic neurons that were wake/REM active, maximally active during REM and maximally active during wake, as we did. They did not record any wake-max GABAergic neurons, however. This discrepancy could be caused by the difference in species, slight differences in recording location or selection bias in the monitored neurons introduced by either the virus expression in the GAD2-IRES-cre mice or blind extracellular recording techniques. It is also possible that even though the head restrained rats had some ability to move, the restraint meant they were unable to move freely. Given that much of the wake activity in the imaged ROIs occurred with high levels of EMG activity, perhaps the changes in firing rate during wakefulness recorded in head restrained rats were underestimated.

In conclusion, each neuronal class is comprised of neurons that were significantly modulated by the sleep-wake cycle and changes in the activity of GABAergic and glutamatergic neurons precede the global behavioral transitions

in brain state. This supports a role for the GABAergic, glutamatergic and cholinergic neurons of the LDT region in the modulation of brain state; specifically in the regulation of REM and wake.

Chapter 4. Discussion

4.1 Preface

Cholinergic signaling in the pons and medulla has been shown to be important for the induction and maintenance of arousal and REM sleep through decades of pharmacology, microdialysis and lesion studies (Baghdoyan, Rodrigo-Angulo, et al. 1984b; George et al. 1964; Kodama et al. 1990; Yamamoto et al. 1990). The brainstem nuclei thought to be the source of this acetylcholine are the laterodorsal tegmental nucleus (LDT) and the pedunculopontine nucleus (PPT) (Jones 2008). These nuclei contain non-cholinergic neurons as well (Clements & Grant 1990; Ford et al. 1995; Wang & Morales 2009), and the experiments reported in chapters two and three sought to determine the sleep-wake activity profiles of the GABAergic and glutamatergic neurons that are intermingled with the cholinergic neurons of the LDT. To accomplish this we took advantage of recent developments in *in vivo* calcium imaging that allowed, for the first time, the monitoring of changes in calcium activity of multiple, identified single neurons in the brainstem. The activity of glutamatergic, GABAergic and cholinergic neurons was significantly modulated by the sleep-wake cycle, with changes in activity preceding global changes in brain state measured with cortical electroencephalography (EEG) and neck electromyography (EMG). In the GABAergic and glutamatergic populations we saw heterogeneity of sleep-wake activity profiles and were able to characterize a positional gradient in the REM or wake selectivity of their responses by assessing the anatomical positions of imaged ROIs. These results indicate that in addition to the cholinergic neurons of the LDT, the GABAergic and glutamatergic neurons are involved in the modulation of the sleep-wake cycle and that there is likely some anatomical organization to their activity.

4.2 Sleep-wake activity of LDT neurons

Imaging the calcium dynamics of brainstem cholinergic neurons across the sleep-wake cycle reveals a pattern of activity that agrees with previous electrophysiological studies of the LDT (Boucetta et al. 2014; Datta & Siwek 2002; Sakai 2012). The activity of these neurons is significantly elevated during REM and wake compared to NREM sleep. Unlike the cholinergic neurons, both the GABAergic and glutamatergic neurons have heterogeneous activity profiles. Examination of the sleep-wake activity of glutamatergic and GABAergic LDT neurons allows us to assess whether these systems could be involved in the pontine regulation of REM sleep and arousal.

The confirmed pattern of activation of cholinergic LDT neurons is consistent with the hypothesis that brainstem cholinergic activity is important for

the cortical desynchronization that occurs during both sleep and wakefulness via projections to the thalamus, hypothalamus and basal forebrain. Intriguingly, acetylcholine activity in the brainstem seems to be important for the induction of REM-specific processes as well (Baghdoyan, Monaco, et al. 1984a; George et al. 1964; Gnadt & Pegram 1986). This indicates that during wake there is some downstream inhibition of acetylcholine's REM-specific actions. Early theories of REM sleep generation posited that the monoaminergic systems in the brainstem were primarily responsible for this inhibition (Hobson et al. 1975; Karczmar et al. 1970; Williams & Reiner 1993). However, more recent pharmacology experiments show that inhibition of GABAergic signaling in the REM-promoting sublaterodorsal tegmental nucleus (SLD) of rats is sufficient to induce REM sleep as well, while application of GABA or GABA receptor agonists increases wakefulness (Boissard et al. 2002; Pollock & Mistlberger 2003; Sanford et al. 2003). This suggests a REM-off population of GABAergic neurons that inhibits the SLD during wake.

We found that the majority of imaged GABAergic neurons (68.6%) were maximally active during periods of arousal. Therefore, it is possible that they are involved in the inhibition of REM-on structures during wakefulness to prevent the expression of REM-specific behaviors. In addition, it is possible that their activity is more specifically wake promoting, perhaps through disinhibition of wake-active structures such as the noradrenergic locus coeruleus (LC). It is unlikely that the LDT GABAergic neurons are responsible for inhibition of the cholinergic neurons during sleep because none of the GABAergic ROIs had significantly elevated activity during NREM sleep.

In contrast to the GABAergic neurons, only 3.5% of the imaged glutamatergic ROIs were wake-max. Instead the largest group of glutamatergic ROIs were maximally active during REM sleep (40.4%). Previous work has shown that injection of glutamate agonists into the SLD causes REM sleep (Boissard et al. 2002; Lai & Siegel 1988), suggesting the presence of REM-on glutamatergic neurons that project to the SLD. The activity profile of the glutamatergic ROIs from the present work is consistent with this hypothesized REM-on glutamatergic population, suggesting that the glutamatergic LDT neurons may be involved in the excitation of REM-promoting structures. Tracing studies have shown that, along with cholinergic projections, glutamatergic LDT neurons project to the pontine regions involved in the induction of muscle atonia through both cholinergic and glutamatergic mechanisms (Lai et al. 1993).

Previous experiments have also predicted the existence of a REM-on population of GABAergic neurons that are responsible for inhibiting REM-off structures such as the monoaminergic nuclei (Gervasoni et al. 1998; Nitz & Siegel 1997). We observed another subset of LDT GABAergic ROIs that were classified as REM-max (13.3%). This REM-selective pattern of activation indicates that GABAergic LDT neurons could provide some of this inhibition.

The remaining glutamatergic (30.7%) and GABAergic (18.1%) LDT neurons increased their activity during both wake and REM sleep, similarly to the

cholinergic neurons. It is possible that, along with the cholinergic cells, these neurons are involved in the cortical desynchronization that occurs during REM and wake. Supporting this role, non-cholinergic, ascending projections along both the ventral and dorsal ascending reticular activating pathways (Figure 1.2) have been identified (Ford et al. 1995; Paré et al. 1988; Semba et al. 1990; Steriade et al. 1988). Non-cholinergic LDT neurons also send descending projections along with the cholinergic neurons to regions important for REM sleep generation (Lai et al. 1993; Semba et al. 1990). Although the details of the cell-type-specific projections from the LDT are still unknown, the similarity of their activity pattern and projection pattern suggests that GABAergic and glutamatergic LDT activity may complement the cholinergic REM and wake promoting actions.

Figure 4.1 incorporates the activity of non-cholinergic LDT neurons into the model proposed in Figure 1.3, delineating hypothetical interactions between various REM-promoting or inhibiting systems based on the sleep-wake activity patterns of these neurons.

4.3 LDT activity during brain state transitions

Further support for the idea that non-cholinergic LDT neurons are important for brain state regulation comes from the finding that changes in their activity precede changes in global brain state determined with EEG and EMG recordings. On average, both glutamatergic and GABAergic ROIs increase their activity several seconds before transitions into wake from either REM or NREM sleep. Glutamatergic and GABAergic ROIs also increase their activity before transitions from NREM into REM and decrease their activity prior to transitions from wake into NREM. This suggests that changes in glutamatergic and GABAergic activity may be causally related to the induction of REM sleep and wake.

Additionally, the increase in GABAergic activity before transitions into wake occurs significantly earlier than transitions in glutamatergic activity. This could support the hypothesis that LDT GABAergic neurons are in part responsible for the inhibition of the REM-specific output of wake/REM excitatory neurons. First, we can hypothesize that the glutamatergic wake/REM ROIs of the LDT belong to the population of neurons involved in both REM and wake induction. If part of what happens during transitions into wake is that the downstream, selectively REM-promoting targets of wake/REM cells are being inhibited to prevent the expression of REM-specific features, then according to this data, the LDT GABAergic inhibition is online before the glutamatergic activity increases around the transition into wake.

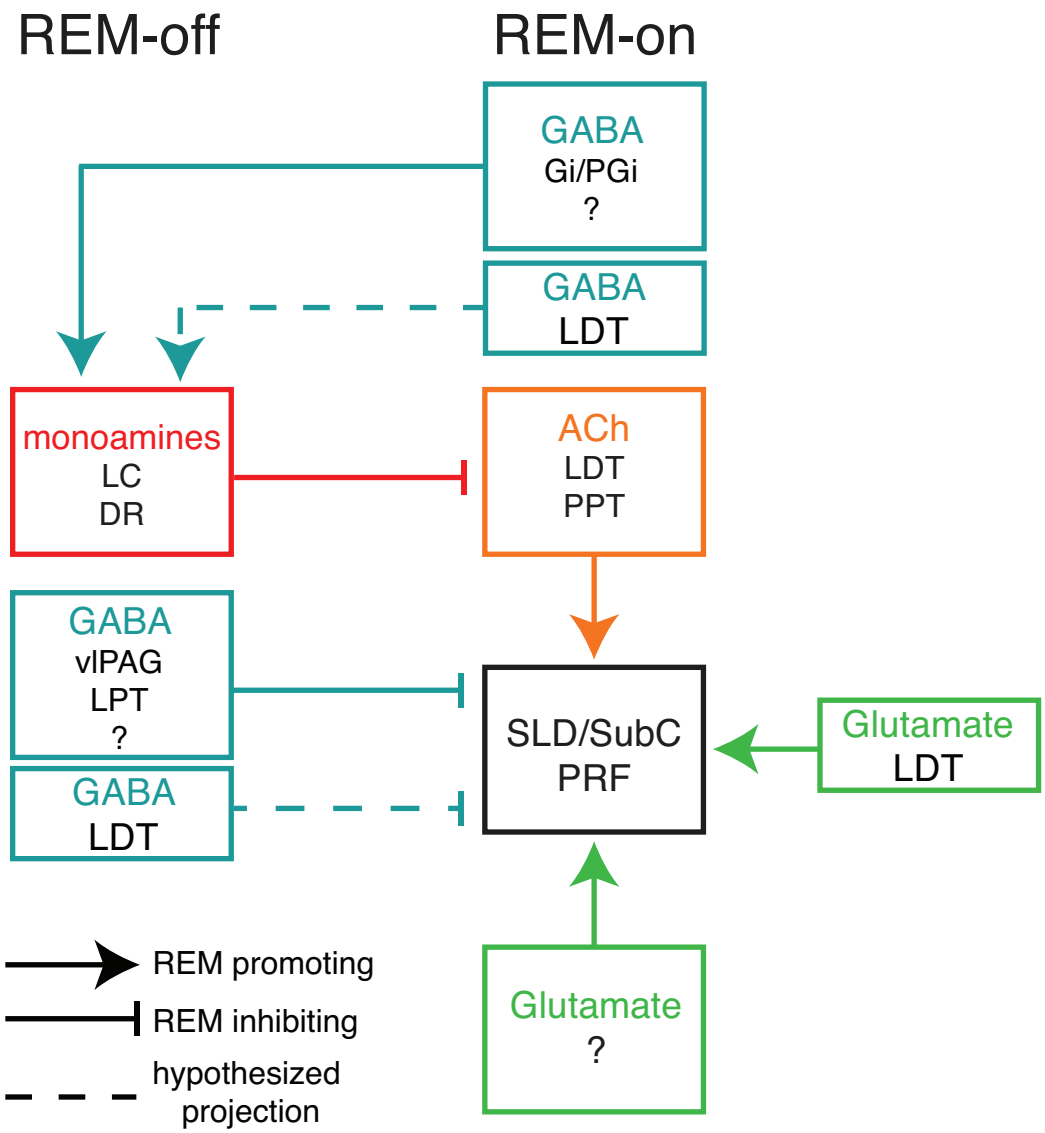

Figure 4.1: Schematic of REM-off and REM-on neurotransmitter actions including hypothesized roles for the non-cholinergic LDT neurons based on their sleep-wake activity profiles. ACh: acetylcholine; DR: dorsal raphe; Gi: gigantocellular reticular nucleus; LC: locus coeruleus; LDT: laterodorsal tegmental nucleus; LPT: lateral pontine tegmentum; PGi: paragigantocellular nucleus; PPT: pedunculopontine tegmental nucleus; PRF: pontine reticular formation SLD: sublaterodorsal tegmental nucleus; SubC: subcoeruleus; vlPAG: ventrolateral periaqueductal gray

4.4 Spatial organization of LDT sleep-wake activity

Calcium imaging affords the unique opportunity to monitor the activity of multiple ROIs simultaneously and then determine whether there is any spatial

organization of their brain state specific activity. Given that all of the ROIs increased their activity during REM, wake or both, we looked at the REM versus wake activity as a function of position for both the glutamatergic and GABAergic ROIs. Although many glutamatergic ROIs were comparably active during both REM and wake, more medially positioned ROIs tended to be more selectively active during REM sleep compared to the more lateral ROIs. Furthermore, both the anterior and posterior extremes of the imaging field were dominated by REM-selective neurons whereas the more central ROIs were similarly active during REM and wake. The GABAergic ROIs also varied in their selectivity. The GABAergic ROIs increased their wake selectivity in more posterior regions compared to more anterior, but did not show much mediolateral organization. Generally, it seems that the more medial and posterior segments of the LDT region are more selectively active during either REM or wake compared to the more lateral and anterior regions, which show relatively comparable levels of REM and wake activity. It will be important to know whether these neurons are synaptically connected with one another; perhaps the GABAergic wake-selective neurons are responsible for the inhibition of the glutamatergic REM-selective neurons during wakefulness.

4.5 Future directions

Cholinergic involvement in REM sleep induction: An important next question is to determine how significant cholinergic activity is for REM sleep induction in rodents. Although decades of research implicate brainstem cholinergic activity in the regulation of REM sleep in cats, experiments that have tried to replicate these canonical experiments in rodents have found inconsistent results. Some groups see increases in REM sleep with infusion of the cholinergic agonist carbachol into midbrain and/or pontine regions (Gnadt & Pegram 1986; Marks & Birabil 1998), while others do not (Boissard et al. 2003). Because these are all microinjection experiments it is possible that the regions analogous to the cat REM-induction sites have not been adequately localized. Perhaps this is in part because brainstem structures in the rodent are so much smaller than in the cat, and pharmacological manipulations are difficult to restrict spatially. Given the increase in activity of cholinergic LDT neurons during REM reported in this dissertation and elsewhere (Boucetta et al. 2014, Sakai 2012), it is probable that cholinergic activity is still important for REM sleep in rodents. One way to assess the sufficiency of brainstem cholinergic activity in REM sleep generation is to optogenetically stimulate the brainstem cholinergic cells located in the LDT and PPT by specifically expressing channelrhodopsin-2 (a cation channel sensitive to blue light) in ChAT positive neurons (Boyden et al. 2005). Because these neurons are active during wake as well, it is possible that stimulation under different conditions may have different effects. Increased cholinergic activity alone may not be sufficient to induce REM, but may need to occur simultaneously with decreased activity in wake-promoting nuclei (Karczmar et al. 1970).

Induction of REM may require that the mouse be in NREM sleep at the time of stimulation. Therefore, it would be interesting to stimulate these cells during various conditions and determine any differential effects on brain state. It is also possible that by stimulating cholinergic fibers in different target regions of these brainstem cholinergic cells we may be able to see different features of REM sleep. For instance, stimulation of the fibers in the thalamus or hypothalamus is likely to induce cortical desynchronization whereas stimulation of fibers in the SLD or medulla may be more likely to induce muscle atonia.

The role of LDT GABAergic neurons in the sleep-wake cycle: Previous studies have predicted the existence of two populations of GABAergic neurons important for the pontine regulation of REM. One population is REM-on and promotes REM via inhibition of wake promoting neurons such as the noradrenergic cells of the LC. The other is REM-off and suppresses REM-promoting structures like the SLD. In our recordings, the majority of GABAergic neurons in the LDT were wake-max. To determine whether they form part of the predicted REM-off GABAergic population, we could optogentically inhibit these neurons using either halorhodopsin or archaerodopsin (chloride and proton pumps, respectively, activated by yellow-green light) (Han & Boyden 2007; Zhang et al. 2007). If they are providing REM-inhibiting GABAergic input to the SLD as predicted by pharmacology experiments (Boissard et al. 2002), then inhibition of these neurons should increase the amount of REM sleep. These pharmacology experiments also suggest that activating the GABAergic neurons would increase wakefulness. Of course, some of these neurons are active during both REM and wake and are perhaps involved in the induction of cortical desychronization. In fact, preliminary data shows that optogenetic stimulation of GABAergic neurons in the LDT region does result in increased desynchronization of cortical EEG. GAD2-cre mice were injected with AAV2-EF1a-DIO-hChR2-EYFP (UNC) to allow for specific expression of channelrhodopsin in the GABAergic neurons of the LDT region. EEG activity was recorded in the freely moving mouse and the GABAergic neurons were stimulated for 5 sec with 473 nm laser. GABAergic stimulation caused a rapid decrease in low frequency activity that persisted for about 10 seconds after the offset of the light, suggesting that stimulation of pontine GABAergic neurons is sufficient to induce cortical desynchronization (Figure 4.2).

Determination of the precise role of these GABAergic neurons will depend on the identification of the projections of these neurons. If they project to structures in the medulla thought to inhibit the LC, they are likely involved in the promotion of wake via disinhibition of monoaminergic activity. If they project to the SLD perhaps they are involved in the inhibition of REM sleep and if they project along the ascending reticular activating system they may be involved in the cortical activation necessary for REM and wake. Given that the GABAergic

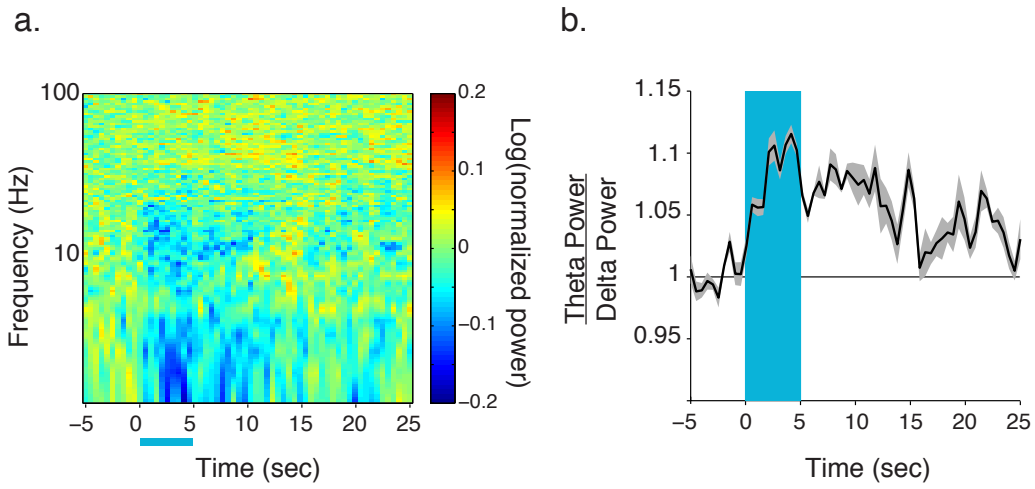

Figure 4.2: Stimulation of GABAergic neurons in the LDT region induces cortical desynchronization

neurons are a somewhat heterogeneous population they may be important for several of these functions. In this case it would be revealing to stimulate the GABAergic LDT fibers in the target structures to see if these different putative outcomes could be dissociated.

It will also be important to identify the targets of the glutamatergic neurons in the LDT. Although they have not been as extensively studied as the cholinergic projections there is some evidence that the glutamatergic LDT neurons project to the subC along with the cholinergic neurons. This, along with their primarily REM-max or wake/REM active discharge profile suggests that they may provide some of the glutamatergic drive to the REM-promoting SLD (Boissard et al. 2002; Lai & Siegel 1988). Thus optogenetic stimulation of both the cell bodies in the LDT and fibers in identified target regions would be vital to the understanding of their role in the pontine REM-promoting circuitry.

The presence of spatial organization of the glutamatergic and GABAergic ROIs in terms of their preference for REM or wake suggests the possibility that targeting optogenetic stimulation to the anterolateral versus the posteromedial regions of the LDT would have different effects on brain state. In the anterolateral area where both the GABAergic and glutamatergic neurons are equally active in REM and wake, the neurons may be more involved in cortical activation. In this case, stimulation would be expected to induce cortical desynchronization irrespective of sleep state. On the other hand, in the posteromedial region the GABAergic neurons are more wake selective and the glutamatergic neurons are more REM selective. Thus, stimulation of the former may induce wakefulness more specifically, while the latter would induce REM sleep.

Finally, the determination of the long-range inputs to these different classes of neurons will be vital to the understanding of how their activity fits into the broader circuitry underlying the regulation of REM and wake.

4.7 Conclusion

Although many studies have elucidated multiple regions and neurotransmitter systems of the brainstem in the modulation of brain state, the precise sleep-wake activity of specific subpopulations of neurons has been difficult to determine. Calcium imaging from specific populations of neurons in deep brain structures in the freely moving mouse provides a powerful tool to dissect the circuitry underlying brainstem control of the sleep-wake cycle. Furthermore, imaging from multiple neurons simultaneously allows for more precise determination of the spatial relationships among multiple neurons and the mapping of any functional organization within subpopulations. With these tools, this dissertation shows that GABAergic, glutamatergic and cholinergic neurons of the laterodorsal tegmental nucleus in the brainstem have distinct and heterogeneous patterns of sleep-wake activity. Furthermore, the activity of GABAergic and glutamatergic neurons anticipate changes in global brain state and vary depending on the cell's position within the LDT.

References

Adey, W.R., Bors, E. & Porter, R.W., 2008. EEG Sleep Patterns After High Cervical Lesions in Man. *Archives of Neurology*, 19(4), pp.377–383.

Armstrong, D.M. et al., 1983. Distribution of cholinergic neurons in rat brain: demonstrated by the immunocytochemical localization of choline acetyltransferase. *The Journal of comparative neurology*, 216(1), pp.53–68.

Aserinsky, E. & Kleitman, N., 1953. Regularly occurring periods of eye motility, and concomitant phenomena, during sleep. *Science (New York, N.Y.)*.

Aston-Jones, G. & Bloom, F.E., 1981a. Activity of norepinephrine-containing locus coeruleus neurons in behaving rats anticipates fluctuations in the sleep-waking cycle. *The Journal of neuroscience : the official journal of the Society for Neuroscience*, 1(8), pp.876–886.

Baghdoyan, H.A., Monaco, A.P., et al., 1984a. Microinjection of neostigmine into the pontine reticular formation of cats enhances desynchronized sleep signs. *The Journal of pharmacology and experimental therapeutics*, 231(1), pp.173–180.

Baghdoyan, H.A., Rodrigo-Angulo, M.L., et al., 1984b. Site-specific enhancement and suppression of desynchronized sleep signs following cholinergic stimulation of three brainstem regions. *Brain research*, 306(1-2), pp.39–52.

Barretto, R. & Schnitzer, M.J., 2012. In vivo optical microendoscopy for imaging cells lying deep within live tissue. *Cold Spring Harbor Protocols*.

Berridge, C.W., 2008. Noradrenergic modulation of arousal. *Brain Research Reviews*, 58(1), pp.1–17.

Boissard, R. et al., 2003. Localization of the GABAergic and non-GABAergic neurons projecting to the sublaterodorsal nucleus and potentially gating paradoxical sleep onset. *The European journal of neuroscience*, 18(6), pp.1627–1639.

Boissard, R. et al., 2002. The rat ponto-medullary network responsible for paradoxical sleep onset and maintenance: a combined microinjection and functional neuroanatomical study. *The European journal of neuroscience*, 16(10), pp.1959–1973.

Borbély, A.A. & Neuhaus, H.U., 1979. Sleep-deprivation: Effects on sleep and EEG in the rat. *Journal of Comparative Physiology ? A*, 133(1), pp.71–87.

Boucetta, S. et al., 2014. Discharge Profiles across the Sleep-Waking Cycle of

Identified Cholinergic, GABAergic, and Glutamatergic Neurons in the Pontomesencephalic Tegmentum of the Rat. *Journal of Neuroscience*, 34(13), pp.4708–4727.

Boyden, E.S. et al., 2005. Millisecond-timescale, genetically targeted optical control of neural activity. *Nature neuroscience*, 8(9), pp.1263–1268.

Brown, R.E. et al., 2012. Control of sleep and wakefulness. *Physiological reviews*, 92(3), pp.1087–1187.

Burgess, C.R. & Peever, J.H., 2013. A Noradrenergic Mechanism Functions to Couple Motor Behavior with Arousal State. *Current Biology*, 23(18), pp.–1725.

Cardin, J.A., 2012. Dissecting local circuits in vivo: Integrated optogenetic and electrophysiology approaches for exploring inhibitory regulation of cortical activity. *Journal of physiology, Paris*.

Carter, M.E. et al., 2010. Tuning arousal with optogenetic modulation of locus coeruleus neurons. *Nature neuroscience*, 13(12), pp.1526–1533.

Cedarbaum, J.M. & Aghajanian, G.K., 1978. Afferent projections to the rat locus coeruleus as determined by a retrograde tracing technique. *The Journal of comparative neurology*, 178(1), pp.1–15.

Chen, T.-W. et al., 2013. Ultrasensitive fluorescent proteins for imaging neuronal activity. *Nature*, 499(7458), pp.295–300.

Cirelli, C. & Tononi, G., 2008. Is Sleep Essential? *PLoS biology*, 6(8), p.e216.

Clements, J.R. & Grant, S., 1990. Glutamate-like immunoreactivity in neurons of the laterodorsal tegmental and pedunculopontine nuclei in the rat. *Neuroscience letters*, 120(1), pp.70–73.

Clément, O. et al., 2011. Evidence that neurons of the sublaterodorsal tegmental nucleus triggering paradoxical (REM) sleep are glutamatergic. *Sleep*, 34(4), pp.419–423.

Cornwall, J. & Phillipson, O.T., 1988. Afferent projections to the parafascicular thalamic nucleus of the rat, as shown by the retrograde transport of wheat germ agglutinin. *Brain research bulletin*, 20(2), pp.139–150.

Dahlström, A. & Fuxe, K., 1964. Localization of monoamines in the lower brain stem. *Experientia*, 20(7), pp.398–399.

Datta, S. & Siwek, D.F., 2002. Single cell activity patterns of pedunculopontine tegmentum neurons across the sleep-wake cycle in the freely moving rats.

Journal of Neuroscience Research, 70(4), pp.611–621.

Economo, Von, C., 1930. Sleep as a problem of localization. *The Journal of nervous and mental disease*.

Foote, S.L., Bloom, F.E. & Aston-Jones, G., 1983. Nucleus locus ceruleus: new evidence of anatomical and physiological specificity. *Physiological reviews*, 63(3), pp.844–914.

Ford, B. et al., 1995. GABAergic neurons in the rat pontomesencephalic tegmentum: Codistribution with cholinergic and other tegmental neurons projecting to the posterior lateral hypothalamus. *The Journal of comparative neurology*, 363(2), pp.177–196.

Fuller, P. et al., 2011. Reassessment of the structural basis of the ascending arousal system. *The Journal of comparative neurology*, 519(5), pp.933–956.

George, R., Haslett, W.L. & Jenden, D.J., 1964. A cholinergic mechanism in the brainstem reticular formation: Induction of paradoxical sleep. *International Journal of Neuropharmacology*, 3(6), pp.541–IN1.

Gervasoni, D. et al, 2004. Global Forebrain Dynamics Predict Rat Behavioral States and Their Transitions. *Journal of Neuroscience*, 24(49), pp.11137–11147.

Gervasoni, D. et al., 1998. Electrophysiological evidence that noradrenergic neurons of the rat locus coeruleus are tonically inhibited by GABA during sleep. *The European journal of neuroscience*, 10(3), pp.964–970.

Ghosh, K.K. et al., 2011. Miniaturized integration of a fluorescence microscope. *Nature Methods*, 8(10), pp.871–878.

Gilbert, C.D. & Sigman, M., 2007. Brain States: Top-Down Influences in Sensory Processing. *Neuron*, 54(5), pp.677–696.

Gnadt, J.W. & Pegram, G.V., 1986. Cholinergic brainstem mechanisms of REM sleep in the rat. *Brain research*, 384(1), pp.29–41.

Goutagny, R. et al., 2008. Role of the dorsal paragigantocellular reticular nucleus in paradoxical (rapid eye movement) sleep generation: a combined electrophysiological and anatomical study in the rat. *Neuroscience*, 152(3), pp.849–857.

Hallanger, A.E. et al., 1987. The origins of cholinergic and other subcortical afferents to the thalamus in the rat. *The Journal of comparative neurology*, 262(1), pp.105–124.

Han, X. & Boyden, E.S., 2007. Multiple-color optical activation, silencing, and desynchronization of neural activity, with single-spike temporal resolution. *PloS one*, 2(3), p.e299.

Helmchen, F. & Denk, W., 2005. Deep tissue two-photon microscopy. *Nature Methods*, 2(12), pp.932–940.

Hobson, J., McCarley, R. & Wyzinski, P., 1975. Sleep cycle oscillation: reciprocal discharge by two brainstem neuronal groups. *Unknown*, 189(4196), pp.55–58.

Holstege, J.C. & Kuypers, H.G., 1987. Brainstem projections to spinal motoneurons: an update. *Neuroscience*, 23(3), pp.809–821.

Huber, R., Deboer, T. & Tobler, I., 2000. Effects of sleep deprivation on sleep and sleep EEG in three mouse strains: empirical data and simulations. *Brain research*, 857(1-2), pp.8–19.

Huber, R. et al., 2004. Sleep homeostasis in Drosophila melanogaster. *Sleep*, 27(4), pp.628–639.

Hurley, L., Devilbliss, D. & Waterhouse, B., 2004. A matter of focus: monoaminergic modulation of stimulus coding in mammalian sensory networks. *Current opinion in neurobiology*, 14(4), pp.488–495.

Issa, E.B. & Wang, X., 2008. Sensory responses during sleep in primate primary and secondary auditory cortex. *Journal of Neuroscience*, 28(53), pp.14467–14480.

Jones, B.E., 2008. Modulation of Cortical Activation and Behavioral Arousal by Cholinergic and Orexinergic Systems. *Annals of the New York Academy of Sciences*, 1129(1), pp.26–34.

Jones, B.E. & Yang, T.-Z., 1985. The efferent projections from the reticular formation and the locus coeruleus studied by anterograde and retrograde axonal transport in the rat. *The Journal of comparative neurology*, 242(1), pp.56–92.

Jouvet, M., 1967. Neurophysiology of the states of sleep. *Physiological reviews*.

Karczmar, A.G., Longo, V.G. & Scotti de Carolis, A., 1970. A pharmacological model of paradoxical sleep: The role of cholinergic and monoamine systems. *Physiology & behavior*, 5(2), pp.175–182.

Kaur, S. et al., 2013. Glutamatergic Signaling from the Parabrachial Nucleus Plays a Critical Role in Hypercapnic Arousal. *Journal of Neuroscience*,

33(18), pp.7627–7640.

Kayama, Y., Ohta, M. & Jodo, E., 1992. Firing of “possibly” cholinergic neurons in the rat laterodorsal tegmental nucleus during sleep and wakefulness. *Brain research*, 569(2), pp.210–220.

Kerlin, A.M. et al., 2010. Broadly Tuned Response Properties of Diverse Inhibitory Neuron Subtypes in Mouse Visual Cortex. *Neuron*, 67(5), pp.858–871.

Kodama, T., Lai, Y.Y. & Siegel, J.M., 1998. Enhanced glutamate release during REM sleep in the rostromedial medulla as measured by in vivo microdialysis. *Brain research*, 780(1), pp.178–181.

Kodama, T., Takahashi, Y. & Honda, Y., 1990. Enhancement of acetylcholine release during paradoxical sleep in the dorsal tegmental field of the cat brain stem. *Neuroscience letters*.

Koyama, Y. & Sakai, K., 2000. Modulation of presumed cholinergic mesopontine tegmental neurons by acetylcholine and monoamines applied iontophoretically in unanesthetized cats. *Neuroscience*, 96(4), pp.723–733.

Krenzer, M. et al., 2011. Brainstem and Spinal Cord Circuitry Regulating REM Sleep and Muscle Atonia. *PloS one*, 6(10), p.e24998.

Krukoff, T.L., 1998. c-fos Expression as a Marker of Functional Activity in the Brain: Immunohistochemistry. In *Cell neurobiology techniques*. New Jersey: Humana Press, pp. 213–230.

Lai, Y.Y. & Siegel, J.M., 1988. Medullary regions mediating atonia. *The Journal of neuroscience*.

Lai, Y.Y., Clements, J.R. & Siegel, J.M., 1993. Glutamatergic and cholinergic projections to the pontine inhibitory area identified with horseradish peroxidase retrograde transport and immunohistochemistry. *The Journal of comparative neurology*, 336(3), pp.321–330.

Lee, A.M. et al., 2014. Identification of a brainstem circuit regulating visual cortical state in parallel with locomotion. *Neuron*, 83(2), pp.455–466.

Lee, S.-H. & Dan, Y., 2012. Neuromodulation of Brain States. *Neuron*, 76(1), pp.209–222.

Loughlin, S.E., Foote, S.L. & Bloom, F.E., 1986. Efferent projections of nucleus locus coeruleus: topographic organization of cells of origin demonstrated by three-dimensional reconstruction. *Neuroscience*, 18(2), pp.291–306.

Lovett-Barron, M. et al., 2014. Dendritic Inhibition in the Hippocampus Supports Fear Learning. *Science (New York, N.Y.)*, 343(6173), pp.857–863.

Lu, J. et al., 2006. A putative flip-flop switch for control of REM sleep. *Nature*, 441(7093), pp.589–594.

Luppi, P.-H. et al., 2006. Paradoxical (REM) sleep genesis: the switch from an aminergic-cholinergic to a GABAergic-glutamatergic hypothesis. *Journal of physiology, Paris*, 100(5-6), pp.271–283.

Luppi, P.H. et al., 1995. Afferent projections to the rat locus coeruleus demonstrated by retrograde and anterograde tracing with cholera-toxin B subunit and Phaseolus vulgaris leucoagglutinin. *Neuroscience*, 65(1), pp.119–160.

Malcolm, L.J., Watson, J.A. & Burke, W., 1970. PGO waves as unitary events. *Brain research*.

Marks, G.A. & Birabil, C.G., 1998. Enhancement of rapid eye movement sleep in the rat by cholinergic and adenosinergic agonists infused into the pontine reticular formation. *Neuroscience*, 86(1), pp.29–37.

Marrosu, F. et al., 1995. Microdialysis measurement of cortical and hippocampal acetylcholine release during sleep-wake cycle in freely moving cats. *Brain research*.

Matsuzaki, M., 1969. Differential effects of sodium butyrate and physostigmine upon the activities of para-sleep in acute brain stem preparations. *Brain research*.

McGinty, D.J. & Harper, R.M., 1976. Dorsal raphe neurons: depression of firing during sleep in cats. *Brain research*, 101(3), pp.569–575.

Monti, J.M., 2011. Serotonin control of sleep-wake behavior. *Sleep medicine reviews*, 15(4), pp.269–281.

Moruzzi, G. & Magoun, H.W., 1949. Brain stem reticular formation and activation of the EEG. *Electroencephalography and Clinical Neurophysiology*, 1(1-4), pp.455–473.

Nitz, D. & Siegel, J.M., 1997. GABA release in the locus coeruleus as a function of sleep/wake state. *Neuroscience*, 78(3), pp.795–801.

Paré, D. et al., 1988. Projections of brainstem core cholinergic and non-cholinergic neurons of cat to intralaminar and reticular thalamic nuclei. *Neuroscience*, 25(1), pp.69–86.

Peters, A. J., Chen, S. X., & Komiyama, T. (2014). Emergence of reproducible spatiotemporal activity during motor learning. *Nature*, *510*(7504), 263–267.

Pinto, L. et al., 2013. Fast modulation of visual perception by basal forebrain cholinergic neurons. *Nature neuroscience*, 16(12), pp.1857–1863.

Pollock, M.S. & Mistlberger, R.E., 2003. Rapid Eye Movement Sleep induction by microinjection of the GABA-A antagonist bicuculline into the dorsal subcoeruleus area of the rat. *Brain research*, 962(1-2), pp.68–77.

Poulet, J.F. & Petersen, C.C., 2008. Internal brain state regulates membrane potential synchrony in barrel cortex of behaving mice. *Nature*, 454(7206), pp.881–885.

Reddy, V.K. et al., 1989. Spinally projecting noradrenergic neurons of the dorsolateral pontine tegmentum: a combined immunocytochemical and retrograde labeling study. *Brain research*, 491(1), pp.144–149.

Robinson, T.E., Kramis, R.C. & Vanderwolf, C.H., 1977. Two types of cerebral activation during active sleep: relations to behavior. *Brain research*, 124(3), pp.544–549.

Sagar, S., Sharp, F. & Curran, T., 1988. Expression of c-fos protein in brain: metabolic mapping at the cellular level. *Science (New York, N.Y.)*, 240(4857), pp.1328–1331.

Sakai, K., 2012. Discharge properties of presumed cholinergic and noncholinergic laterodorsal tegmental neurons related to cortical activation in non-anesthetized mice. *Neuroscience*, 224(C), pp.172–190.

Sakai, K. et al., 1977. Afferent projections to the cat locus coeruleus as visualized by the horseradish peroxidase technique. *Brain research*, 119(1), pp.21–41.

Sanford, L.D. et al., 2003. GABAergic regulation of REM sleep in reticularis pontis oralis and caudalis in rats. *Journal of neurophysiology*, 90(2), pp.938–945.

Sapin, E. et al., 2009. Localization of the brainstem GABAergic neurons controlling paradoxical (REM) sleep. *PloS one*, 4(1), p.e4272.

Sara, S.J., 2009. The locus coeruleus and noradrenergic modulation of cognition. *Nature reviews Neuroscience*, 10(3), pp.211–223.

Semba, K., Reiner, P.B. & Fibiger, H.C., 1990. Single cholinergic mesopontine tegmental neurons project to both the pontine reticular formation and the thalamus in the rat. *Neuroscience*, 38(3), pp.643–654.

Shiromani, P.J. et al., 1992. Cholinergically induced REM sleep triggers Fos-like immunoreactivity in dorsolateral pontine regions associated with REM sleep. *Brain research*, 580(1-2), pp.351–357.

Shouse, M.N. & Siegel, J.M., 1992. Pontine regulation of REM sleep components in cats: integrity of the pedunculopontine tegmentum (PPT) is important for phasic events but unnecessary for atonia during REM sleep. *Brain research*, 571(1), pp.50–63.

Siegel, J., REM sleep anatomy and physiology.

Siegel, J., 2013. REM Sleep Anatomy and Physiology. In K. C, ed. *The Encycopedia of Sleep*. Elsevier, pp. 460–472.

Siegel, J.M., 2005. Clues to the functions of mammalian sleep. *Nature*, 437(7063), pp.1264–1271.

Siegel, J.M., Nienhuis, R. & Tomaszewski, K.S., 1984. REM sleep signs rostral to chronic transections at the pontomedullary junction. *Neuroscience letters*.

Siegel, J.M., Tomaszewski, K.S. & Nienhuis, R., 1986. Behavioral states in the chronic medullary and midpontine cat. *Electroencephalography and clinical neurophysiology*.

Steriade, M., 2004. Acetylcholine systems and rhythmic activities during the waking-sleep cycle. *Progress in brain research*, 145, pp.179–196.

Steriade, M. & Glenn, L.L., 1982. Neocortical and caudate projections of intralaminar thalamic neurons and their synaptic excitation from midbrain reticular core. *Journal of neurophysiology*, 48(2), pp.352–371.

Steriade, M. et al., 1988. Projections of cholinergic and non-cholinergic neurons of the brainstem core to relay and associational thalamic nuclei in the cat and macaque monkey. *Neuroscience*, 25(1), pp.47–67.

Steriade, M., Oakson, G. & Ropert, N., 1982. Firing rates and patterns of midbrain reticular neurons during steady and transitional states of the sleep-waking cycle. *Experimental brain research*, 46(1), pp.37–51.

Takahashi, K. et al., 2010. Locus coeruleus neuronal activity during the sleep-waking cycle in mice. *Neuroscience*, 169(3), pp.1115–1126.

Timo-Iaria, C. et al., 1970. Phases and states of sleep in the rat. *Physiology & behavior*, 5(9), pp.1057–1062.

Triarhou, L.C., 2006. The percipient observations of Constantin von Economo on encephalitis lethargica and sleep disruption and their lasting impact on

contemporary sleep research. *Brain research bulletin*, 69(3), pp.244–258.

Van Twyver, H., 1969. Sleep patterns of five rodent species. *Physiology & behavior*, 4(6), pp.901–905.

Vanini, G. et al., 2011. Endogenous GABA levels in the pontine reticular formation are greater during wakefulness than during rapid eye movement sleep. *The Journal of Neuroscience*

Verret, L. et al., 2005. Cholinergic and noncholinergic brainstem neurons expressing Fos after paradoxical (REM) sleep deprivation and recovery. *The European journal of neuroscience*, 21(9), pp.2488–2504.

Vertes, R.P., 1984. Brainstem control of the events of REM sleep. *Progress in neurobiology*, 22(3), pp.241–288.

Vyazovskiy, V.V. et al., 2011. Local sleep in awake rats. *Nature*, 472(7344), pp.443–447.

Wang, H.-L. & Morales, M., 2009. Pedunculopontine and laterodorsal tegmental nuclei contain distinct populations of cholinergic, glutamatergic and GABAergic neurons in the rat. *The European journal of neuroscience*, 29(2), pp.340–358.

Webster, H.H. & Jones, B.E., 1988. Neurotoxic lesions of the dorsolateral pontomesencephalic tegmentum-cholinergic cell area in the cat. II. Effects upon sleep-waking states. *Brain research*.

Williams, J.A. & Reiner, P.B., 1993. Noradrenaline hyperpolarizes identified rat mesopontine cholinergic neurons in vitro. *The Journal of neuroscience*.

Woolf, N.J. & Butcher, L.L., 1989. Cholinergic systems in the rat brain: IV. descending projections of the pontomesencephalic tegmentum. *Brain research bulletin*, 23(6), pp.519–540.

Wu, M.F. et al., 1999. Locus coeruleus neurons: cessation of activity during cataplexy. *Neuroscience*, 91(4), pp.1389–1399.

Xi, M.C., Morales, F.R. & Chase, M.H., 1999. Evidence that wakefulness and REM sleep are controlled by a GABAergic pontine mechanism. *Journal of neurophysiology*, 82(4), pp.2015–2019.

Xi, M.-C., Morales, F.R. & Chase, M.H., 2004. Interactions between GABAergic and cholinergic processes in the nucleus pontis oralis: neuronal mechanisms controlling active (rapid eye movement) sleep and wakefulness. *Journal of Neuroscience*, 24(47), pp.10670–10678.

Yamamoto, K. et al., 1990. A cholinoceptive desynchronized sleep induction zone in the anterodorsal pontine tegmentum: Spontaneous and drug-induced neuronal activity. *Neuroscience*.

Zhang, F. et al., 2007. Multimodal fast optical interrogation of neural circuitry. *Nature*, 446(7136), pp.633–639.

Ziv, Y. et al., 2013. Long-term dynamics of CA1 hippocampal place codes. *Nature neuroscience*, 16(3), pp.264–266.